Beyond Power: Bedrock River Incision Process and Form

Gregory S. Hancock and Robert S. Anderson

Department of Earth Sciences, University of California, Santa Cruz, California

Kelin X Whipple

Department of Earth, Atmospheric, and Planetary Sciences, MIT, Cambridge, Massachusetts

We present a quantitative discussion of the processes active in bedrock-floored river channels, drawn from field observations, erosion rate measurements, and simple scaling rules. Quantitative documentation of process is needed to improve our understanding of bedrock river channels and aid in the formulation of erosion rules to be used in landscape evolution simulations. Our observations in a channel with "hard" rock (Indus River, Pakistan) suggest quarrying and abrasion are the primary erosion processes. It appears that block quarrying is the most efficient process when joints and bedding planes are sufficiently close. The block thickness a river is capable of quarrying goes as the square of the local flow velocity, v. Quarrying requires block "preparation", during which subaerial weathering, bedload bashing, and/or hydraulic wedging, a previously undocumented process, act to free a block for quarrying. The Indus River is capable of quarrying blocks of up to ~0.7 m during annual peak flows. Rock abrasion should go as $\sim v^5$. Abrasion is most effective in regions of separated flow, generating a suite of sculpted rock bedforms that includes flutes, and this suggests abrasion occurs primarily by suspended sediment. Cavitation is unlikely to be a major process, as it requires unusually high velocity, and is suppressed by flow aeration. Abrasion measured on the Indus over 1 year using drill holes is ≤4 mm, with maximum rates within flutes, and in locally steep, narrow channel segments. Cosmogenic radionuclides from the same bed locations reveal average erosion rates over ~1.5-2.0 ka that are an order of magnitude lower than the maximum 1 year rates. We reconcile these measurements by appealing to the passage of bedforms such as flutes. Our Indus River rate measurements are many times lower than longer-term rates, possibly implying substantial hydrologic variation induced by climate change. Incision rates in bedrock channels are controlled by very local hydraulic conditions well below the resolution of reach-based erosion rules. Incorporation of this geometric complexity represents a significant challenge to the landscape evolution modeling community.

1. INTRODUCTION

1.1 *Why Study Bedrock River Channels?*

Bedrock channels and the erosional forms found in them are some of the most glorious features on Earth. They provide the primary non-glacial mechanism of incision into

Rivers Over Rock: Fluvial Processes in Bedrock Channels
Geophysical Monograph 107

the bedrock of tectonically active regions. This incision steepens bounding hillslopes and produces relief between the mountain tops and the channel bottom, and removes mass from mountain ranges, leading to flexural isostatic response that can drive the uplift of peaks [e.g., *Small and Anderson*, 1995; *England and Molnar*, 1990]. Bedrock channel incision provides the essential link between tectonics and landscape evolution, through communication of base level changes through the landscape. The rate at which channels incise into bedrock sets the rate at which the rest of the landscape surface evolves, and hence controls the response time of such landscapes to tectonic and/or climatic forcing.

That the role of bedrock rivers in landscape evolution is central requires that we be able to predict properly bedrock channel incision and profile development in models attempting to simulate landscape evolution [*Howard et al.*, 1994]. "Rivers" in such models must be able to respond to changes induced climatically (e.g., stream discharge, hillslope sediment production) or tectonically (e.g., changes in gradient due to tilting, baselevel changes), and to variations in substrate (e.g., rock hardness) that in turn dictate the available erosion processes. A complete model for bedrock channel evolution should be flexible enough to incorporate these variables in a meaningful way.

However, bedrock rivers remain a poorly understood part of the geomorphic system. In an attempt to understand these features more fully, we have undertaken a field study to assess quantitatively the processes that are active in bedrock rivers. In this paper, we start by discussing the existing models for predicting erosion rates in bedrock channels. Much of the recent research interest in bedrock rivers stems from the need for model development, and by discussing these models we highlight the necessity of reconsidering field evidence to understand these systems. We then discuss our field observations of processes (abrasion, quarrying/hydraulic wedging, and cavitation) that are potentially important in the bedrock rivers in which we have worked. For each process, we attempt to develop a quantitative expression that allows us to discuss how process efficiency might vary with hydraulic and channel characteristics. We then discuss how these processes potentially interact in these systems and influence channel shape and profile evolution. Finally, we discuss our direct, short-term measurements of abrasion on the Indus River, northern Pakistan, and the implications these rates have for erosion in this and other channels is accomplished.

1.2. *Modeling Bedrock Channel Erosion*

The effort to understand how bedrock channels work is motivated in part from interest in treating these features in landscape evolution models [e.g., *Howard et al.*, 1994]. Physical "rules" developed to predict rock channel erosion rates build on either an erosion process, which we term "process rules", or reach-averaged expressions of erosive capacity, which we term "reach-scale rules". Process rules are attractive because they 1) develop a physically-based understanding of individual processes; and 2) allow direct estimation of how erosion by that process might vary with changing hydraulic and sediment load conditions. However, if the goal is to use a physical rule in a numerical simulation of channel profile development or landscape evolution, the typical time and length scales of such simulations will likely preclude direct calculation of the parameters (e.g., flow velocity, sediment concentration) required for prediction of erosion rates with a process rule. As an alternative, reach-scale rules employ surrogates for erosive capacity, like shear stress and stream power, coupled with a parameter that relates these functions to channel erosion rates. The parameters necessary for calculating erosion rates with these rules, like drainage area and slope, are measured at a map scale, rather than the microphysical scale, making them more computationally efficient than process rules. However, in abstracting the incision processes, we may lose the ability to predict accurately how incision rates might vary in space and time in response to changing conditions, and, hence, the ability to predict accurately the evolution of the profile. We now discuss in detail the "process" and "reach-scale" rules.

1.2.1. *Process rules. Foley* [1980a] outlines the only published, well-developed "process rule" for predicting erosion rates in bedrock channels. *Foley* [1980a] develops his model for cutting and deformation abrasion of bedrock by bedload impact, and tests this model using measured (e.g., grain size) and estimated (e.g., discharge, rock susceptibility) parameters against field-determined incision rates. He builds on *Allen* [1971] by using the engineering wear literature for prediction of volume loss from a rock surface as a function of kinetic energy delivery by impacts. The removal of material of a rock surface (i.e., erosion, or wear), *dz/dt*, produced by this kinetic energy delivery is expressed as

$$\frac{dz}{dt} = \frac{1}{2}\frac{C_{sed}}{\lambda}\left(\frac{v_g - v_0}{S_a}\right)^2 \qquad (1)$$

where C_{sed} is the bedload sediment concentration, l is the saltation hop length for the bedload, v_g is the particle velocity perpendicular to the bed, v_0 is the threshold particle velocity necessary for initiation of erosion, and S_a is the "susceptibility" of the rock relating kinetic energy delivered to mass of rock removed [*Foley*, 1980a].

Abrasion rates predicted by this model are highly sensitive to the flow hydrograph. *Foley* [1980a] estimates that flows representing only a small fraction (<0.05%) of the annual hydrograph could account for all of the long-term average incision at his field site (Dearborn River, Montana). He emphasizes the importance of hydrograph changes produced by climate cycling (here,

interglacial/glacial cycles) on erosion rates. Two critical implications of the nonlinearity of Eq. 1 and the quantitative field analysis by *Foley* [1980a] are 1) while there is a tradeoff of flow frequency and magnitude, the highest flows are likely the most important in accomplishing erosional wear of the bed by abrasion, and 2) long term changes in the details of the stream hydrograph and in sediment concentration can strongly influence bedrock incision rates.

This equation is very limited in application to quite specific channel types, as *Foley* [1980a] very clearly describes, precluding broad use of this rule. This arises from the need to know the local C_{sed}, v_g, and v_0 in order to predict *dz/dt*. Such quantities cannot be predicted efficiently or confidently in a long-term model simulating drainage basin evolution, because information about these quantities is difficult to extract from the geologic record. In addition, abrasion by bedload impacts as outlined in Eq. 1 is not the predominant process in all places or even in one place at all times, requiring that rules be developed for other processes, and that we understand how to predict which process dominates at a particular time or place.

1.2.2. *Reach-scale rules.* The "reach-scale rules" move away from explicitly addressing a process, and instead rely on relationships between map-scale (100's m to many km) measurable quantities and erosion rate. These rules start with either shear stress, τ,

$$\tau = \rho g S_e H \tag{2}$$

as in *Howard and Kerby* [1983], or "specific" stream power, ω,

$$\omega = \frac{\rho_w g S_e Q}{w} \tag{3}$$

where ρ_w is the density of water, g is gravitational acceleration, Q is water discharge, w is channel flow width, S_e is energy slope, and H is flow depth (equal to hydraulic radius for wide, shallow streams). Erosion rules that utilize these as a starting point explicitly assume, in the case of shear stress, $dz/dt \sim t$, or, in the case of stream power, $dz/dt \sim w$, where *dz/dt* is the average erosion rate at a point. With these assumptions, we can develop an erosion rate law that is a function of discharge, Q. We use the Darcy-Weisbach equation for mean flow velocity, $\bar{v}$,

$$\bar{v} = \left(\frac{8 g S_e H}{f} \right)^{1/2} \tag{4}$$

where f is the Darcy-Weisbach friction factor, and the continuity equation, $Q = \bar{v} H w$, to relate Q to S_e and H. Combining these with Eq. 2, we obtain a shear stress-based rule,

$$\frac{dz}{dt} = K_1 \frac{Q^{1/3} S_e^{2/3}}{w^{2/3}} \tag{5}$$

where K_1 is a constant. Combining these with Eq. 3, we obtain a stream power-based rule,

$$\frac{dz}{dt} = K_2 \frac{Q S_e}{w} \tag{6}$$

where K_2 is a constant.

In landscape evolution models, addressing the specifics of discharge and channel width are difficult at large spatial and temporal scales, particularly given the stochastic variation of Q over long time scales. A solution is suggested by *Howard and Kerby* [1983], and reviewed by *Howard et al.* [1994], who argue that the long term average incision rate is proportional to the shear stress exerted by the "dominant discharge" in the channel [*Costa and O'Connor*, 1995; *Wolman and Miller*, 1960]. *Howard and Kerby* [1983] suggest drainage area, A_D, as a surrogate for this dominant discharge, and develop an equation for estimating channel erosion rates,

$$\frac{dz}{dt} = K A_D^m S^n \tag{7}$$

where K is a constant, S is channel bottom slope (replacing S_e), and m and n are exponents that depend on the choice of shear stress or stream power as the erosion surrogate. Although K is frequently referred to as a channel resistance term, this is not strictly correct; K folds in many factors, including but not limited to rock resistance, that are sensitive to the erosional process and setting [e.g., *Stock and Montgomery*, in press; Figure 1].

Several studies have attempted to calibrate the parameters m, n, and K in Eq. 7 with field data. *Howard et al.* [1994] suggest using the empirical relationships $Q_b \sim A_D^b$, where Q_b is the bankfull discharge and b ranges from ~0.65 to ~0.80, and $w \sim Q^{(0.5)}$, both determined from drainage basins with primarily alluvial channels [*Leopold et al.*, 1964; *Knighton*, 1984]. It is an important and often unstated assumption that bedrock channels have similar relationships between Q and w and A_D; these relationships have not been empirically determined for any bedrock river system, and defining a "bankfull" discharge in most bedrock rivers is inherently impossible. Using these empirical relationships, one obtains m=0.2 to 0.3 and n=2/3 for a shear stress rule, and m=0.3 to 0.4 and n=1 for a stream power rule. In both formulations, the final erosion

rate is not as strongly dependent on Q as channel slope, S. This results from the dependence of both w and Q on A_D. Using measurements of erosion rates, and of channel slopes and drainage area for badland channels, *Howard and Kerby* [1983] find the best-fitting values, m=0.45 and n=0.70, similar to what is expected by following a shear stress development. Several studies have attempted to calibrate K, m, and n in the field [e.g., *Rosenbloom and Anderson*, 1994; *Seidl and Dietrich*, 1992; *Seidl et al.*, 1994; *Stock and Montgomery*, in press], with highly variable results.

Rate laws similar to Eq. 7 are used extensively in landscape and stream profile evolution models to study how landscapes respond to tectonics and climate change [e.g., *Howard*, 1994; *Tucker and Slingerland*, 1997]. A major drawback in this rate law, however, is that most factors that are relevant to the variability of incision rates in a particular setting are folded into the K parameter, which is not readily estimated because it subsumes such a large number of variables (Figure 1). It is also possible that channel erosion rates change with changing hydrologic forcing through time (e.g., through changing climate), or with changes in dominant processes along a channel reach. As written, a rate law like Eq. 7 cannot explicitly incorporate such variability in either time or space, unless K is allowed to vary in some meaningful way, because A_D is fixed for a particular channel location.

We also note that Eq. 6, the origin of the stream power erosion rule, implies no dependence of erosion rates on the shape of the hydrograph. For an annual hydrograph passing a point in the channel, the integrated stream power (effectively, the total potential energy loss of the water) is always equal regardless of the details of the flow hydrograph. Unlike microphysical rules, like Eq. 1, this implies erosion rates are insensitive to the hydrograph shape, unless a threshold stream power for erosion exists.

1.3. *Stepping Back: Field Investigation of Bedrock Rivers*

We think that improving our understanding of bedrock channels requires more direct field observations of the processes that actually operate in these channels. Attempts to develop and calibrate reach-scale rules have motivated much of the recent quantitative research related to bedrock channels [e.g., *Howard*, 1987; *Howard et al.*, 1994; *Howard and Kerby*, 1983; *Seidl and Dietrich*, 1992; *Seidl et al.*, 1994; *Sklar and Dietrich*, 1997; *Slingerland et al.*, 1997; *Stock and Montgomery*, in press]. In contrast, recent field studies tend to focus either on individual processes or bedforms [e.g., *Foley*, 1980a; *Miller*, 1991; *Nemec et al.*, 1986; *Tinkler*, 1993; *Zen and Prestegaard*, 1994] or on reach-scale energy expenditure in bedrock channels and related channel form [e.g., *Ashley et al.*, 1988; *Wohl*, 1992; *Wohl*, 1993; *Wohl et al.*, 1994]. These process studies have not been directed towards model development (with the exception of *Foley* [1980a]), and have not provided estimates of process rates.

We have gone to the field, with simulation models in mind but understanding processes a priority, in a quantitative investigation of which processes are active, what scales the rates of these processes, how these processes interact, and how fast these processes act. Our observations of sculpted rock bedforms and channel morphology demonstrate that incision into bedrock is not accomplished by any single process, but through a linked and interconnected set of physical processes that vary in their efficacy from place to place and from time to time. In this paper, we present an overview of the incision processes we observe to be most critical (abrasion, quarrying) or potentially important (cavitation) in eroding "hard" bedrock channels. For each, we attempt to develop a simple, conceptual process model, and a mathematical expression that allows scaling of process rates and discussion of where each may be most important. While we do not attempt to develop new "rate laws", we discuss whether existing reach-scale rate laws are appropriate for particular processes. One of the greatest limiting factors in understanding process in these settings is the lack of rate measurements, given the slow rates at which bedrock channels typically erode. We have directly measured erosion by abrasion on the Indus River, and discuss the results and their relevance to how such a river erodes.

We draw insight from a variety of rivers with different character: 1) the Indus River Middle Gorge, Pakistan, a steep, bedrock-floored river with huge annual swings in discharge, that crosses "hard" igneous and metamorphic rocks amongst some of the most rapidly uplifting topography in the world [*Burbank et al.*, 1996]; 2) the Wind River, which is forced by glacial/interglacial cycling and incises through weak, early Tertiary continental deposits [*Chadwick et al.*, 1997; *Hancock et al.*, 1998]; and 3) several rivers draining the Sierra Nevada, California, which are primarily snow-melt streams running on mixed bedrock ("hard" igneous and metamorphic rocks) and alluvium-mantled beds. We use the Indus River as a test case for estimating process rates, because it is a large river in a tectonically active setting, and we have made measurements of erosion rates on this river.

2. BEDROCK EROSION PROCESSES

We consider in detail abrasion, quarrying/hydraulic wedging, and cavitation. These processes either appear to be very active in the channels we have observed (abrasion and quarrying), or are potentially important (cavitation). While other processes are certainly active in some bedrock river channels (e.g., chemical dissolution), they appear to be less significant in the "hard" rocks that floor the rivers we have considered. We will address the physics and scaling of each process initially, and then discuss where each process is likely most effective. We then consider the interaction among these processes in a conceptual model of bedrock channels.

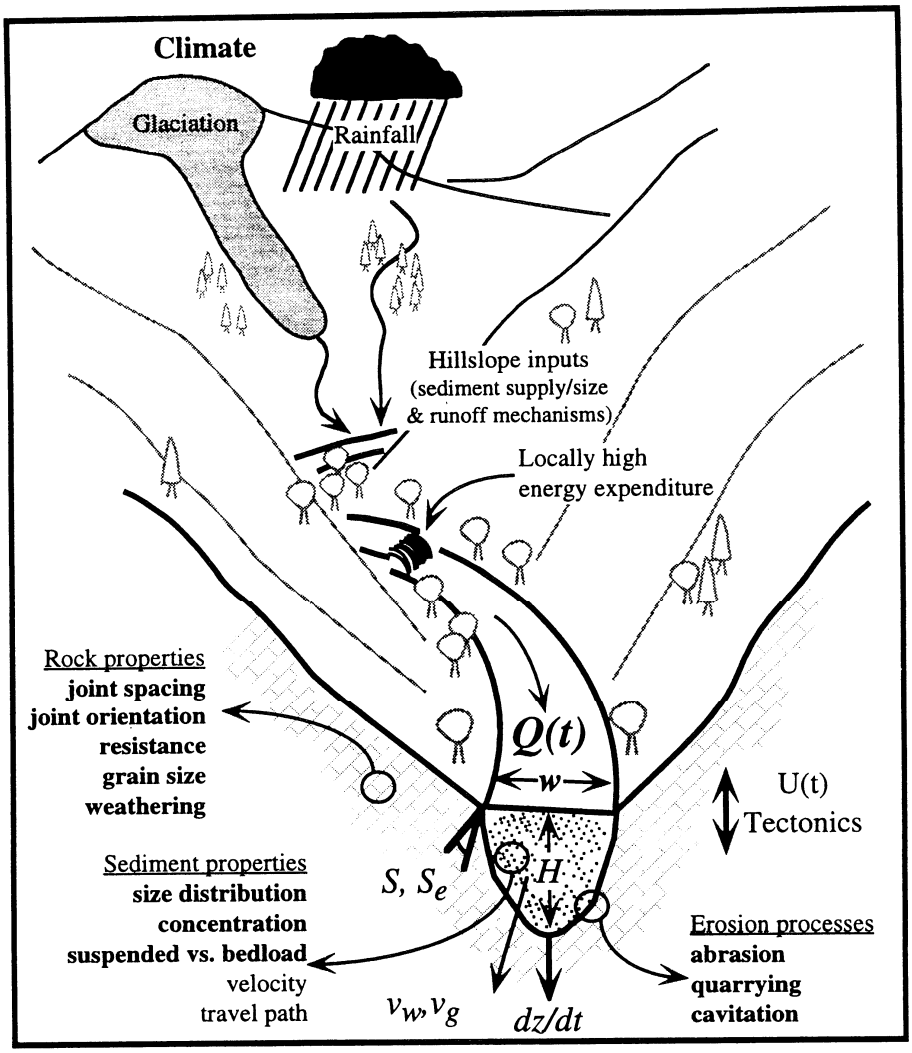

Figure 1. A schematic of a bedrock channel system, showing important variables that act to set the erosion rate, *dz/dt*, of the channel and terms used in the text. Channel variables are: $Q(t)$: discharge as a function of time; w: channel width; H: flow depth; v_w: water velocity; v_g: sediment velocity; A_D: drainage area; and S and S_e: channel and energy slope, respectively. Variables that are at least partially subsumed within the parameter, K, found in all reach-scale erosion rules, are shown in bold.

2.1. *Abrasion*

2.1.1. *Theory*. Rock erosion by abrasion is accomplished by removal of material from a rock surface through forcible impact by entrained sediment. The rate at which material is removed depends upon the kinetic energy flux to the surface, delivered by impacting grains, and the "susceptibility" of the rock surface to abrasion [e.g., *Anderson*, 1986; *Foley*, 1980a]. The impacts produce fractures within minerals, dislodge individual grains, or break off flakes from the rock surface. Experimental studies of abrasion by aeolian sediment transport reveal that the mass of material removed is roughly proportional to the to the kinetic energy delivered by the impact [e.g., *Greeley and Iversen*, 1985; *Suzuki and Takahashi*, 1981]. At the grain scale, the grain velocity, v_g, diameter, D, and density, ρ_g, set its kinetic energy, and the delivery of this kinetic energy increases as grain impact angle, a, relative to the bed, increases toward vertical (90 degrees). The "susceptibility", S_a, relates kinetic energy delivery to mass of rock material removed, and is dependent primarily on the density, hardness, and fracture-mechanical properties of the

target and impacting grains. In a development analogous to aeolian abrasion presented by *Anderson* [1986], we can express, in simple terms, an abrasion erosion rate as

$$\frac{dz}{dt} \sim \frac{S_a C_{sed} v_g^2 v_w}{2\rho_r} \quad (8)$$

where C_{sed} is the mass concentration of a particular grain size, v_w is water flow velocity, and ρ_r is the target rock density, and we have assumed impact by spherical grains. Assuming $v_g \sim v_w$, and a C_{sed} proportional to shear stress ($C_{sed} \sim t \sim v_w^2$), Eq. 8 suggests that $dz/dt \sim v_w^5$. This argues that abrasion rates are very sensitive to local flow conditions and the details of the flow hydrograph, with high local stream velocities and the largest, rare flow events producing the greatest instantaneous erosion rates.

Abrasion rates are sensitive to the grain scale microphysics. The most relevant velocity is the particle velocity, v_g, relative to the channel bed, rather than simply the water flow velocity. For a particle to impact the channel floor, sediment must decouple from the flow, because flow velocity vanishes at the bed. The entrained sediment must possess enough momentum to decouple from the flow, punching through the near-surface flow boundary layer and forcibly impacting the bed. The sediment concentration, C_{sed}, is not sufficient for predicting erosion as presented in Eq. 8. Analogous to aeolian abrasion by suspended sediment *Anderson* [1986], particle trajectories are influenced by the response of water flowlines to the microtopography of the bed. A particle may be steered by the water around obstacles, or be forced to impact the obstacle obliquely if its inertia is sufficiently low. Increased sediment in the flow may actually decrease the rate of erosion as sediment supply begins to choke off access to the bed [*Sklar and Dietrich*, 1997].

Exceedence of a threshold may also be required to initiate erosion by abrasion. A threshold kinetic energy is explicitly included in several abrasion rules, requiring grains exceed either a threshold velocity, v_0, or diameter, D_0 [*Anderson*, 1986; *Foley*, 1980a]. Burial of the bed by sediment at low flow conditions is commonly observed in bedrock channels [e.g., *Howard*, 1987]; sufficient sediment transport and local bed scour is therefore required to remove sediment mantles on the bed before abrasion can take place. Both of these thresholds presumably require surpassing a threshold discharge and/or flow duration. The long-term abrasion rate of a channel will therefore be influenced by climatic changes that change the frequency of exceeding these thresholds.

2.1.2. *Insights from abrasion-related bedforms*. Sculpted rock bedforms like flutes (or "troughs") and potholes represent the most actively abrading portions of a rock bed. Our observations indicate that such forms originate where sharp flow expansions on the downstream edges of bed protrusions allow flow separation with an associated flow recirculation zone. Flow separation occurs where the boundary layer of a stream of viscous fluid detaches itself from the boundary in response to abrupt expansions or adverse pressure gradients, generating a free shear layer with a region of separated flow. These flow separation regions, which are characterized by high water flowline curvature, allow entrained sediment to decouple from the flow and impact the bed. We establish several lines of evidence that argue that the primary tools in accomplishing this abrasion are the suspended grains. The erosional "bedforms" that adorn rock surfaces require that the grains be capable of delivering significant kinetic energy to the back sides of flow obstacles and expansions. Below we illustrate several forms that support this notion that the abrasional "attack is from the back".

We take as a first example the ripple-like bedforms shown in Figure 2, which are many times smaller in amplitude than the flow depth. These are presumably similar to the "hummocky" bed topography described by *Wohl* [1992]. We find these forms are often well developed on the tops of bedrock protrusions, and on the crests of large boulders in the flow. They are especially well developed in fine-grained rocks. We propose that these forms evolve from incipient, low amplitude, long wavelength sinuous ridges in the surface to more sharply crested forms. Once sharp crested, the ridges become ornamented on their downstream sides by subsidiary flutes with near bilateral symmetry in planview (Figure 3) similar to those discussed by *Allen* [1971] in cohesive mud beds, but without a central axial rise [Figure 1d, *Allen*, 1968]. The flutes are often overhanging on the upstream side (Figure 3). The symmetry and overhang argue that the flutes reflect the vortices generated in the zone of flow separation developed at the crest, as suggested for similar features by *Maxson and Campbell* [1940]. We suggest that the high angular acceleration of the flow is capable of flinging high momentum suspended grains energetically out of the vortex and against the bed, causing efficient imprinting of the flow field into the rock form (Figure 3). These flow separation vortices are also spawned by joints, fractures and small bed irregularities, and flutes and potholes are often formed in association with these features. Once growth of these forms is initiated, their presence tends to enhance the flow separation region. The flutes migrate in an upstream direction, like miniature knickpoints, as erosion rates are highest on the upstream, overhanging end of the form (Figure 4), where recirculating flow is focused [*Allen*, 1968]. Flutes appear to occasionally "stall" in their upstream march and develop a more rounded rather than elongated shape (Figure 4). The "stall" may result from changes in the feature or the surrounding bed which diminish the strength of flow separation. Once reaching this morphology, the flute may behave more like a pothole, with erosion focused downward rather than headward as vertical vortices act to selectively erode the flute bottom [*Alexander*, 1932].

A.

B.

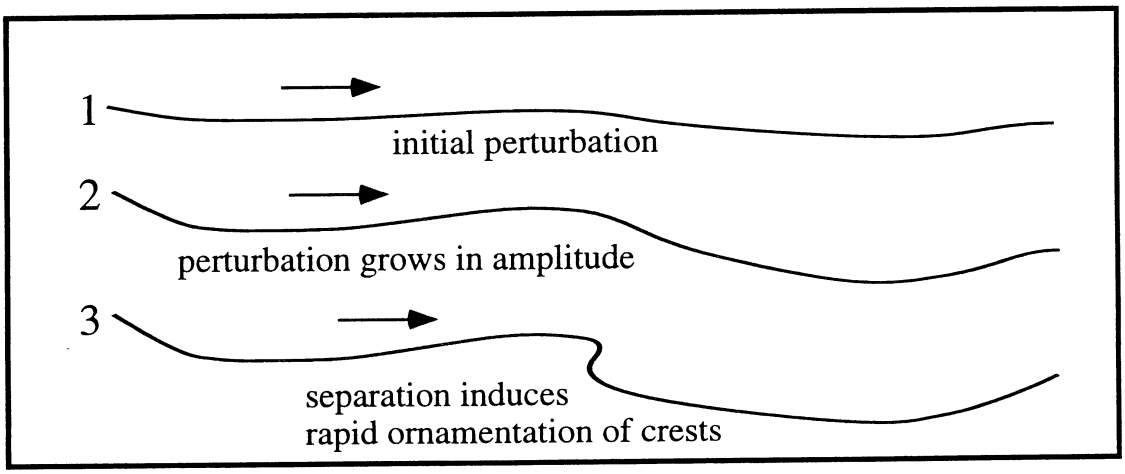

Figure 2. A) Active channel bed on the Indus River (Site H, Figure 10) showing ripple-like bedforms developed in bedrock. Flow direction is from lower left to upper right, and flow covers this bed by many meters during high flow (this is many times the ripple amplitude; note backpack for scale). Note how ripple forms are fairly regularly spaced, grow in amplitude and become more sharp-crested as a drop in the bed (upper limit of visible bed) is approached. Ripples at upper right have grown sufficiently to spawn flutes on their crest, which are effectively incising downward and headward into the rock surface. B) Schematic ripple cross-section, showing initial bed perturbation (1), growth of perturbation through differential bed erosion (2), and ornamentation of the ripple crest by flutes once crest begins to generate flow separation vortices on the downstream side.

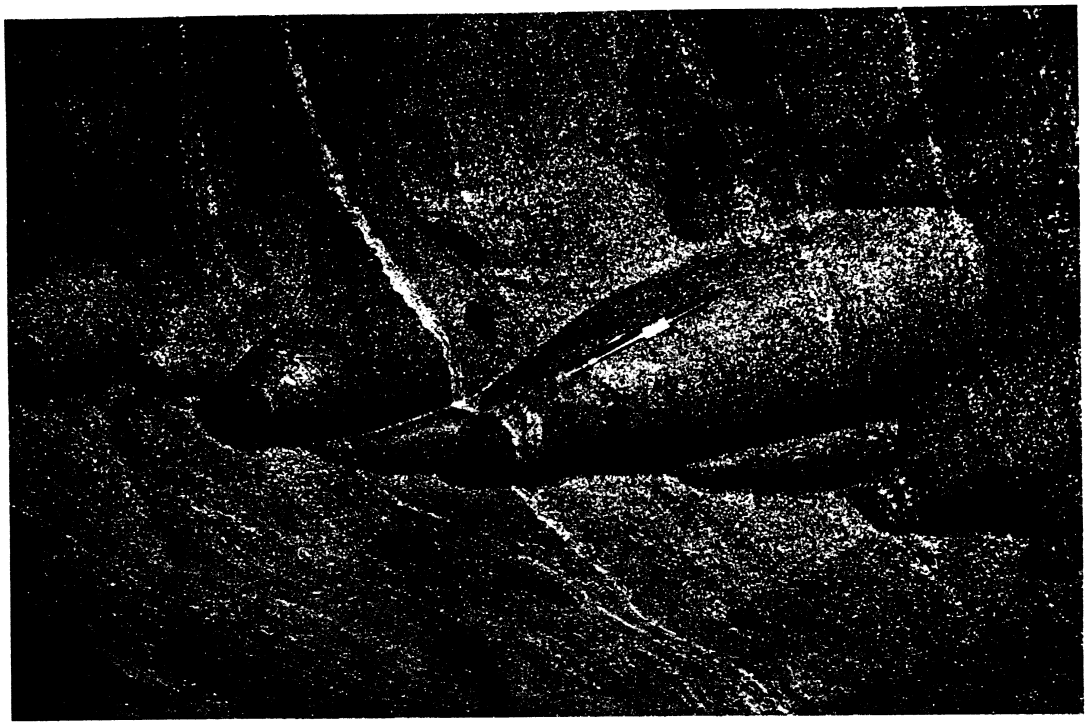

Figure 3. Flutes developed in bedrock on the Indus River (Site C, Figure 10). Flow direction is from top to bottom, in line with pencil (pencil length is ~15 cm). The flutes are nearly symmetrical in planview (note flute containing pencil), and several are overhanging. These flutes are presumably spawned by flow separation vortices generated by an edge on the rock face; these vortices allow effective decoupling of suspended sediment from the flow, and imprinting of the flow field on the rock. Note subordinate flute (small flute to left of flute containing pencil), presumably resulting from vortices shed from the edge of the large flute [*Allen*, 1971], and now eating into the head of the next flute downstream.

We often find that bedrock or boulders that protrude into the flow have a smooth, polished upstream side, a highly etched, fluted flow parallel side, and a heavily fluted, and potholed downstream side (Figure 5; see figures in *Maxson and Campbell* [1940]). We argue that the smooth front surface results from abrasion by suspended sediment, but that the rate of abrasion must be lower than on the flow-parallel and downstream sides, where rock is more rapidly removed in the abrasional bedforms. Because the flow can "feel" an upcoming obstacle at some distance upstream, on the order of several obstacle diameters, the flow field is able to diverge gradually as the obstacle is approached (Figure 6). Flow lines diverge slowly, resulting in low flow curvature and lateral acceleration. The suspended load remains coupled with the flow as it approaches the obstacle. In contrast, in the flow expansion downstream of the obstacle, in bed downdrops, or in fractures, the flow separates if the pressure increase associated with the decelerating flow is sufficient, producing recirculating eddies with extreme flow line curvature. Suspended sediment of sufficient momentum cannot be steered by the flow in such eddies, and may be flung against the bed, generating the "attack from the back". We expect that the larger grain sizes (fine to medium sand in the case of the Indus River) within the suspended load will be most effectively decoupled.

2.2. *Bed Quarrying and Hydraulic Wedging*

2.2.1. Quarrying of blocks. Quarrying, or plucking, of bedrock blocks from the bed is accomplished by lifting or sliding of blocks defined by an existing set of discontinuities in the rock (e.g., joints, fractures, bedding planes). Quarrying is a common and efficient mechanism for lowering bedrock river channels where joint and bedding plane spacing and their dip relative to stream flow direction allow it to be active [e.g., *Miller*, 1991]. Our field observations suggest that quarrying of blocks is the most rapid means of eroding a bedrock channel floor where the

Figure 4. Upstream migrating flutes on horizontal surface on top of a boulder (focus of Figure 5, Indus River, Site C, Figure 10). Flow direction is from left to right, and flow covers this site by up to ~5 m in high flows. Ruler length is ~15 cm. These flutes are spawned by separation along a joint in the rock, which can be seen running from top to bottom, parallel and left of the ruler, and passing the tips of the pen and pencil. Below the lower pen, incipient flutes are currently developing along the joint. Between the pen and pencil, the flutes have migrated upstream (left) and away from the joint surface by up to ~20 cm. Note several flutes directly left of the ruler have become rounded, rather than elongate; these "flutes" may be stalled in their upstream march, evolving into incipient potholes.

joint spacing is sufficiently close to allow blocks to be moved by river flow. We base this hypothesis on observations that 1) in channels where joint or bedding plane spacing allows quarrying, the bed morphology is blocky and is defined by joint or bedding planes, reflecting the removal of blocks; and 2) abrasional flutes and potholes etch only shallowly into the bedrock touching up the corners of the joint blocks, and do not appear to evolve quickly enough to mute the blocky topography.

We develop two simple physical models of bed quarrying to place constraints on the type of flows adequate to quarry blocks. Blocks defined by joint edges or bedding planes may be lifted or slid out of their intact positions by the flow. This is likely preceded by some "preconditioning period" during which the joint surfaces are weathered, wedged apart (e.g., by hydraulic wedging, discussed below), and/or weakened by bashing with bedload. Assuming block removal following this preconditioning proceeds without the need for breaking chemical bonds, the block may be removed by 1) lift generated by pressure differences in the flow, or 2) sliding or rotating in response to the shear stress exerted on the upper block surface.

We first consider a simple hydraulic "lifting" of the block in the case where only the upper surface is exposed to flow. By assuming hydraulic connection between water in the joints and the free flowing water above the bed, we can use the Bernoulli equation to estimate the threshold velocity necessary to lift the block (Figure 7). Joints are assumed to be perfectly horizontal and vertical. The water in the joints will exert a pressure, P_1, on the joint faces, while the free-flowing water above the block will be have pressure, P_2, dictated by the flow velocity, v. To initiate lift of the block, the force difference associated with pressure differences, $(P_1\text{-}P_2)xy$, must be sufficient to overcome the buoyant weight of the joint block, $g(\rho_r\text{-}\rho_w)xyz$, where ρ_r and ρ_w are the density of the bedrock and water, respectively, and x, y, and z are the dimensions of the joint block (Figure 7). Rearranging this equation, we can estimate the threshold velocity, v_t, required to initiate lift of the block,

Figure 5. Boulder illustrating variation in bed erosion with orientation relative to the flow, Indus River. Flow direction is from left to right, and flow covers this site by up to ~5 m in high flows (low-flow stage river is seen in background). Note large boulder left of person is smoothly polished on the upstream side, fluted on the top, flow parallel side (see Figure 4 for detail), and heavily potholed on the downstream side. We argue the smooth front reflects abrasion, but erosion here is at a slower rate than within the flutes and potholes, where flow separation, resulting in high flowline curvature and angular acceleration, allows decoupling of suspended sediment from the flow.

$$v_t \sim \left[\frac{2gz}{\rho_w}(\rho_r - \rho_w)\right]^{1/2} \quad (9)$$

This will be a minimum threshold, as we have ignored the friction against the bounding blocks. The bed-parallel block dimensions, x and y, do not play a role in determining whether a block will be lifted.

An alternate formulation considers that a block is slid out of its intact position by the shear stress acting on the block surface. This scenario is analogous to the degradation of knickpoints described by *Miller* [1991] in carbonate rock-floored streams in southern Indiana. Again, it is likely that the block must be "prepared" by weathering or wedging for some period of time before this process can be activated. In this case, we consider the shear forces, exerted by the shear stress acting at the top of the block in opposition to the frictional forces acting to hold the block in place (Figure 7). Again the joints are assumed to be perfectly horizontal and vertical. In order for a block to slide, the shear force, F_S, must exceed the frictional force, F_F, $\rho_w g S H x y > \mu_s g(\rho_r - \rho_w) x y z$, where μ_s is the coefficient of static friction, and H is the water depth above the block. We again rearrange to derive the dependence of block thickness, z, that can moved on the flow conditions, HS_e,

$$HS_e \sim \frac{z\mu_s}{\rho_w}(\rho_r - \rho_w) \quad (10)$$

The mean flow velocity, v, in a channel goes as $(HS_e)^{1/2}$ (Eq. 4), indicating that for this process $v_t \sim z^{(1/2)}$, or $z \sim v_t^2$ or as in Eq. 9.

We now estimate the potential for maximum block thicknesses quarried under field conditions. In the Indus River, with maximum $S \sim 0.01$ (we substitute S for S_e), $H \sim 10$ m, and shear velocities (u^*)~1 m/sec, we estimate velocities of ~5 m/sec at ~1 m above the bed during high flows. Assuming ρ_r=2.7 g/cm^3 and ρ_w=1.0 g/cm^3, these conditions are sufficient to initiate lift of a block with z~0.7 m (Eq. 9), or, assuming dry rock-to-rock contact (m_s=~0.4), to initiate sliding of a block with z~0.15 m (Eq.

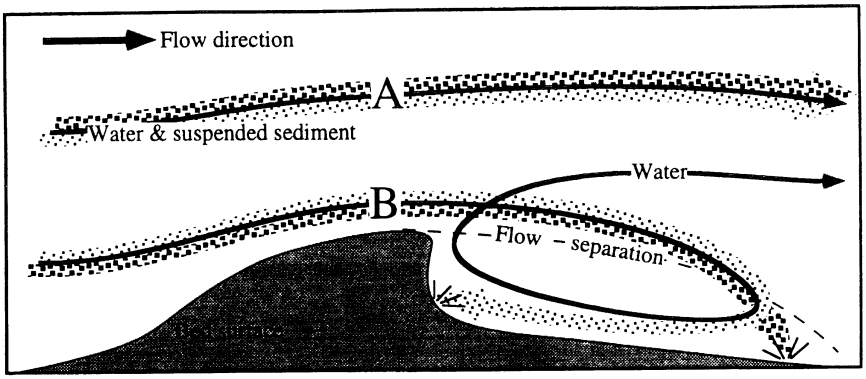

Figure 6. Schematic of flow around a bed obstacle. Flow is from left to right, and two flow lines are shown, A and B. On flowline A, the water and the suspended sediment remain coupled although flow adjusts to passing over the bed obstacle. Following flowline B, sediment and water remain coupled on upstream side of the obstacle, as flowline curvature is relatively slow as the flow approaches the obstacle. However, downstream of the obstacle, flow separation is initiated in response to the flow expansion and adverse pressure gradient. Water recirculates in this region before escaping downstream, but because the flowlines in this region are highly curved, the water flow cannot steer the sediment. The sediment is flung out of the flow and against the bed, with the location of sediment decoupling within the separation region dependent upon the grain size.

10). This estimate for block sliding does not consider possible water lubrication of the joints or assistance by block lift (both effectively lower m_s), both of which will increase potential size of the block which may be moved under these conditions. For both, the dip of the joint planes relative to the horizontal will also enhance or reduce the potential for block motion [*Miller*, 1991].

These expressions suggest that the ability of a river to erode its bed by quarrying increases as the square of velocity, which is expected because both $(P_1\text{-}P_2)$ and t go as v^2. This implies that the largest flows are capable of removing substantially thicker blocks than low flows. We note that in this case the local joint spacing of a channel therefore sets a threshold velocity and, hence, a threshold discharge, Q_t, below which no quarrying can take place. If $Q_t > Q_{max}$, abrasion will be the dominant process. According to Eqs. 9 and 10, with a given discharge through a river reach, quarrying will be enhanced locally where water surface slopes and flow velocities are high, like channel constrictions and steep drops. While not considered in Eqs. 9 and 10, the distribution of joint dip and strike relative to flow direction also controls quarrying rates [*Miller*, 1991]. We have neglected as well the needed "preparation time" of the joint blocks, which introduces a waiting-time threshold to the quarrying process.

2.2.2. *Hydraulic wedging.* We report here another process, previously undocumented, that loosens and prepares blocks for quarrying by wedging clasts into fractures and joints. We have termed this process "hydraulic wedging". We have noted in nearly every setting where joints are found in the bedrock that transported clasts, ranging in size from fine sand to boulders, are wedged very tightly into the joints (Figure 8). Removal of the clasts requires significant force, like a hammer blow, that often shatters the clast before it comes loose. This implies that the clasts are either emplaced forcefully, or are passively inserted as a joint temporarily widens. Forceful emplacement might be accomplished either by very high flow velocities and forceful injection by water, or if clasts possess sufficient momentum to slam into the joints. Both seem unlikely, because flow velocities should be relatively low in joints and even the finest (cm) scale fractures contain wedged grains. Another possibility is bashing of the clasts into joints by larger, saltating bedload particles. Deposited sediment is often not found on the bed outside of the filled joints (Figure 8), implying that sediment is trapped in the joints as it is being transported efficiently across the surface, rather than being "sieved" into the joints as a layer of sediments rests on the bedrock surface. A more likely scenario for clast emplacement may be slight widening of joint faces by pressure fluctuations exerted by the turbulent water flow, temporarily creating space for clasts with dimensions nearly equal to the static joint width. The clasts, if trapped during this temporally widening, act to "ratchet" the joint open through time by preventing the joint relaxation following expansion, or to weaken the joint face as it closes back down on the clast. Opening and widening of the joint will enhance subaerial weathering during low flow conditions, and promote hydraulic communication between the flow above the bed and the joint waters. In this way, hydraulic wedging likely plays an important role in setting the "preparation time" required before blocks can be quarried from the bed. The mechanics of this process are far from understood.

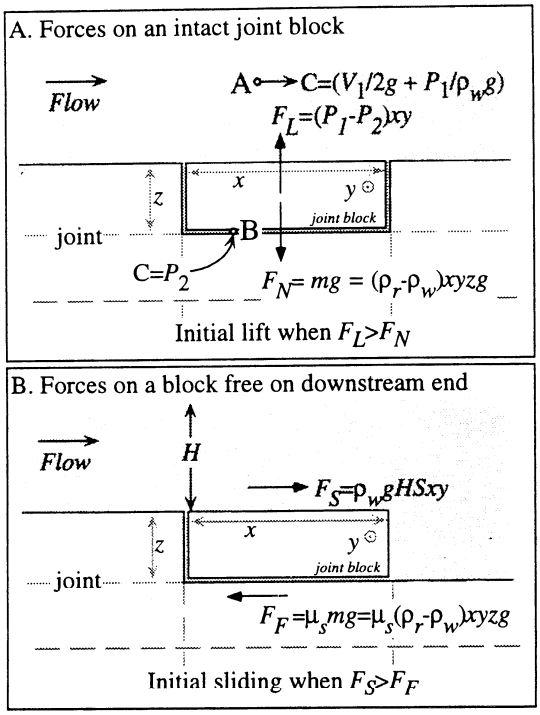

Figure 7. A) Sketch of forces acting on a joint block bounded on all sides except the top, and with dimensions x, y, and z. The total hydraulic head, C, at the two points, A and B, is equal, assuming hydraulic communication between the joint waters and the free-flowing stream, and negligible elevation difference between the points. Lift of the block will be initiated when the lift force, $F_L=(P_2-P_1)xy$, exceeds the buoyant weight of the block, $F_N= g(\rho_r-\rho_w)xyz$. Threshold velocity for initiation of lift for a given block thickness, z, is given in Eq. 9. B) Sketch of forces acting on a joint block bounded on all sides except the top and rear, and with dimensions x, y, and z. Initiation of block motion will occur when the tractive force, $F_S=\rho_w gSHxy$, exceeds the force of frictional resistance, $F_F=\mu g(\rho_r-\rho_w)xyz$. Threshold velocity for initiation of lift for a given block thickness, z, is given in Eq. 10.

2.3 *Cavitation*

Cavitation in water occurs when local flow velocities are sufficiently high to produce small regions in the flow in which pressure falls temporarily below the water vapor pressure. This may occur where flow is constricted and obstructed locally, resulting in increased water velocities [*Barnes*, 1956]. In such regions, water-vapor filled cavities, or bubbles, then form within the flow. As these cavities are advected into regions of higher pressure associated with lower flow velocity, they collapse. During collapse, a powerful microjet of water threads through the bubble [see figure 4-18 in *Hammitt*, 1980]. Although small in size (<mm), these microjets act as miniature water hammers of remarkable strength if they impact a solid surface, and can lead to surface pitting and cracking [see figures in *Barnes*, 1956; *Bourne and Field*, 1995].

While cavitation is clearly a concern in engineered structures (e.g., turbines), it remains unclear whether it plays a role in natural river channels. We attempt herein to determine if conditions necessary for cavitation are likely in a natural bedrock channel. *Barnes* [1956] developed an equation for predicting cavitation in natural channels based on the Bernoulli energy balance equation expressed in terms of hydraulic head,

$$\frac{v_m^2}{2g}+\frac{p_a}{\rho_w g}+z_s=\frac{v_c^2}{2g}+\frac{p_v}{\rho_w g}+z_b \qquad (11)$$

This assumes a constant (mean) velocity, v_m, across the "normal channel cross section" and a local velocity at the point of cavitation, v_c, which is k times higher than the mean flow velocity. The terms p_a and p_v are the atmospheric pressure and the vapor pressure of water, respectively, and z_s and z_b are the elevation at the stream surface and bottom, respectively. Following *Barnes* [1956] and *Wohl* [1992], we make the assumption that $v_c=kv_m$, $z_b=0$, and $z_s=H$ (stream depth), and solve for the mean flow velocity required for cavitation to occur,

$$v_m=\left[\frac{2(p_a-p_v)}{(k-1)\rho_w}+\frac{2gH}{(k-1)}\right]^{1/2} \qquad (12)$$

While probably oversimplified, this equation illustrates that the threshold velocity needed for cavitation initiation in a channel decreases (hence, cavitation likelihood increases) with increasing H, p_v, and ρ_w, and with decreasing p_a.

We now estimate the likelihood of cavitation in a natural channel. With estimates of threshold velocities given by Eq. 12, and assuming near steady and uniform flow conditions to allow substitution of S_e with S, we can predict the channel slope, S, needed to generate cavitation for a given flow depth H by rearranging Eq. 4,

$$S=\left(\frac{f}{8Hg}\right)v_m^2 \qquad (13)$$

where we substitute S for S_e. Figure 9 shows threshold v_m and S values for given flow H assuming a range of 2 to 3 for k, and a range of typical values for S and H found in the Middle Gorge Indus River. The mean stream velocities and slopes for cavitation are quite high relative to typical stream values, even a steep, high discharge river such as the Indus. The v_m and S thresholds are likely exceeded only

Figure 8. Example of clast-filled joints, resulting from hydraulic wedging of clasts. Flow direction is left to right, and reach ~10 m maximum depth at high flow.

in locally steep or narrow reaches along a stream (Figure 9). However, we note that these locally steep reaches are often locations where rapids aerate the flow. Entrained air impedes cavitation by increasing the compressibility of the water. Very little air entrainment is required (roughly 0.3% by volume (*Rasmussen* [1949], cited in *Barnes* [1956]) before cavitation is reduced to a minor or negligible process.

We therefore suspect erosion of rock by cavitation in natural bedrock channels is not significant. We have not observed the pitting or cracking of rock surfaces, which are expected to result from cavitation damage and would tend to roughen the bed surface [*Barnes*, 1956; *Bourne and Field*, 1995]. In addition, the extreme velocities necessary for cavitation are rare, even in a steep river. Unlike many engineered structures, roughness in rivers, like rapids, may substantially aerate the flow, inhibiting cavitation.

2.4. *Processes, Channel Evolution, and Simulations*

The bedrock channels we have investigated erode through the interaction of the processes described above. The most efficient process in any given location depends on the flow conditions (e.g., channel hydraulics, sediment size and load)

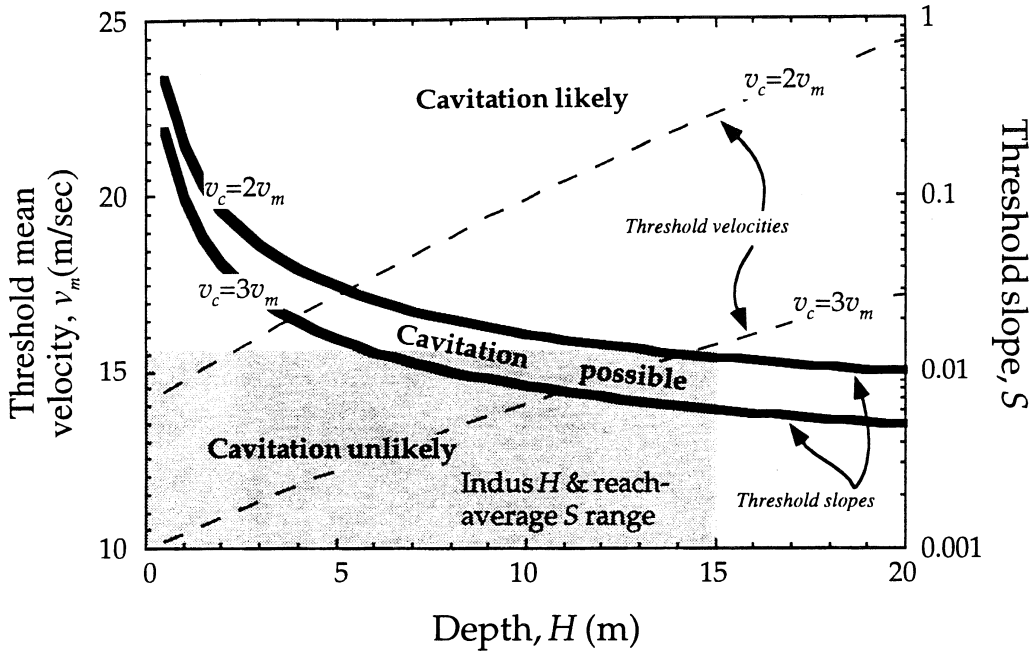

Figure 9. Estimated likelihood of cavitation in the Indus River using Eqs. 12 and 13, and assuming local bottom flow velocities range from 2 to 3 times higher than mean velocities ($3v_m \geq v_c \geq 2v_m$, k=2-3, see Eq. 12). We use the values p_a=101 kPa (sea-level), p_v=1.23 kPa (10°C value for water), ρ_w=1.0 g/cm^3, g=9.8 m/sec^2, and a value for f corresponding to a Manning's n=0.03. Thin dashed lines show threshold mean velocities, v_m, required to produce local bottom velocities, v_c, sufficient to initiate cavitation, with one line for $3v_m=v_c$ and one for $2v_m=v_c$ calculated with Eq. 12. Thick black lines show channel slopes required to generate these mean velocities, calculated using Eq. 13. Below the lower thick black line, slope is insufficient to generate the velocities necessary to produce cavitation at the specified depth; between the thick black lines, slopes and depths are potentially sufficient to drive cavitation; and above the upper thick line, cavitation is likely. The gray box shows the range of typical flow depths and reach-average slopes (over 100's of meters) for the Indus. Cavitation is possible only at the highest flows in the Indus according to the criteria we have selected.

and rock characteristics (e.g., joint spacing, "susceptibility", grain size). Quarrying is most effective where joint blocks are closely spaced enough to allow the available channel flow to quarry them regularly (implied by *Tinkler* [1993]), or for rare events to accomplish substantial quarrying in a short time. The efficiency of this process is not dependent on entrained sediment. The need to prepare the blocks for removal by subaerial weathering and/or hydraulic wedging of joints results in a block "preparation time". Once rocks too massive to be quarried are encountered, abrasion becomes the tool of choice. In a river with generally similar rock susceptibility but variability in joint spacing, we suggest reaches where abrasion is the predominant process must become steeper and narrower relative to the quarried reaches. This provides the additional energy expenditure required by abrasion to keep pace with quarried reaches. If a channel erodes into a massive rock unit that can only be eroded by abrasion, this reach will exert a rate-limiting control on the profile evolution upstream until this reach can steepen and narrow sufficiently, or until the massive rock is sawed through. In these settings, the potential rate-limiting nature of abrasion makes it a critical process to understand.

In all rivers, access to the rock bed is required before rock erosion can take place. Channel incision occurs only when the supply of sediment to the channel cannot keep it constantly mantled. In many bedrock stream systems, bedrock is covered at least partially by sediment [*Howard et al.*, 1994; *Sklar and Dietrich*, 1997]. The flow must therefore be sufficient to allow removal of the sediment cover before erosion can take place. Sediment transport therefore plays a role not only in setting rates of abrasion, but also in clearing the way for erosion to take place. Places where channels narrow and are steeper, with an accompanying increase in flow velocities relative to up- and downstream, may be better able to remain "cleaned" of sediment, allowing enhancement of bed erosion. Differential erosion of such sections may lead to steepening of upstream sections, enhancing sediment capacity and potential for bedrock erosion [*Howard et al.*, 1994].

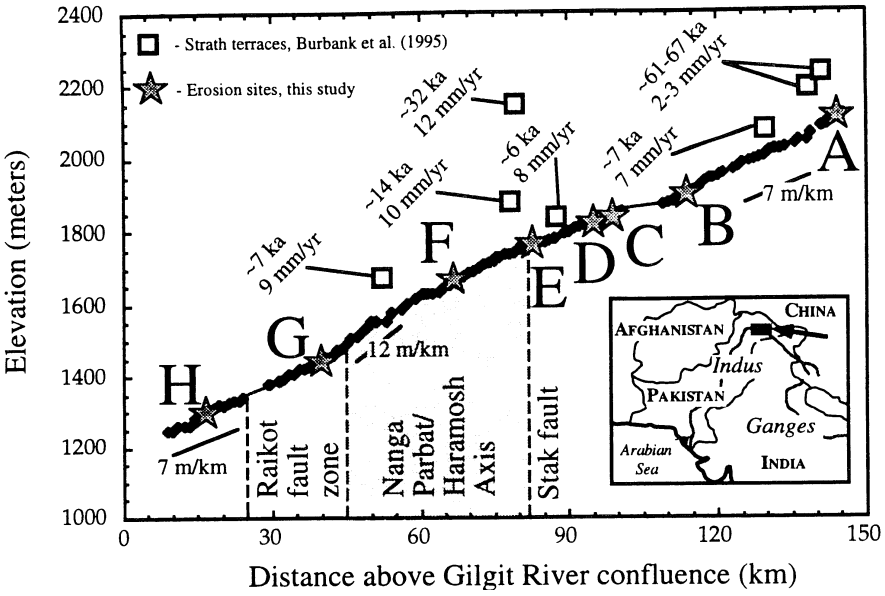

Figure 10. Profile of the Indus River through its Middle Gorge, with inset showing position of Middle Gorge in southern Asia. Each diamond in the profile reflects a survey point along the river. Reach-averaged slopes within the Middle Gorge range from 7 to 12 m/km, and are steepest as the river crosses the Nanga Parbat - Haramosh axis. Open boxes show position, CRN exposure ages (i.e., dates) and mean incision rates since terrace abandonment for strath terraces documented by *Burbank et al.*, 1996. Stars and accompanying letters show the position of the 7 erosion monitoring sites used in this study. The arrow marks the position of the Kachura gauging station at the upper end of the gorge.

Sediment transport needs to be treated in simulations of channel evolution to incorporate realistically the commonly observed bed protection by sediment cover.

The effectiveness of each process is sensitively dependent on flow conditions, and needs consideration in reach-scale models. In all of the expressions above, the process effectiveness scales nonlinearly with flow velocity. This points out the potential importance of large, rare flow events, and the details of the flow hydrograph in a river system [e.g., *Wohl*, 1992]. The "dominant discharge" may be different for each process, and therefore may not be well-characterized by a single choice for discharge surrogate. These are not captured explicitly in erosion rules relying on drainage area as a discharge surrogate. In addition, this sensitivity to velocity, coupled with our observations and measurements (discussed below), strongly suggest reach to sub-reach scale variations in channel width, slope and morphology are critical in setting channel bed erosion rates for each process. Abrupt topographic breaks in the channel long profile ("knickpoints") are examples of such places [e.g., *Howard et al.*, 1994; *Miller*, 1991; *Wohl et al.*, 1994]. A two-fold increase in mean flow velocity, induced by local channel narrowing and/or steepening, can lead to a ~2 to 10 fold increase in erosion rates, following the developments done for each process outlined above. Erosion rules relying on channel slopes calculated over reaches of 100's to 1000's of meters, which are typical length scales in simulation modeling, cannot account for the importance of sub-reach scale variations. Simulation models need to incorporate meaningfully variation of slope and width at scales below the reach scale, or predicted profile evolution may not be realistic.

3.0 FIELD MEASUREMENTS OF ROCK ABRASION RATES, INDUS RIVER

To measure short-term, local incision rates in a very active bedrock channel, we selected seven sites to monitor erosion along a ~150 km stretch of the Middle Gorge of the Indus River (sites A through H, Figure 10; Table 1). This river crosses "hard" metamorphic and igneous rocks throughout the Middle Gorge, and is steep, with reach-averaged slopes up to ~12 m/km (Figure 1). The Indus here has a drainage area of ~100,000 km^2, and has a large average annual swing in discharge from ~300 to >4000 m^3/sec. Maximum discharges during the period of gauging record (1970-1986) are >7500 m^3/sec. *Burbank et al.* [1996] estimated river bed erosion rates of ~1-10 mm/yr over the last ~6 to 70 ka by dating abandoned fluvial strath terraces now tens to hundreds of meters above the river (NPHA,

Table 1. Erosion monitoring site information.

Site	Local village name	Distance above confluence (km)[a]	Rock type	Schmidt hammer test[b]	Slope[c]	Estimated maximum stream power (W/m^2)[d]
A	Kachura	144	schist	65±2.9	0.0073	3800
B	Baghicha	118	granite	60±4.8	0.012	4500
C	Mendi	100	granite	69±1.5	0.0022	850
D	Triku	99	granite	66±1.1	0.0074	1500
E	Stak	83	mica schist	56±2.6	0.0017	800
F	Subsar	68	gneiss	64±2.7	0.02	17000
G	Burumdoir	39	gneiss	60±3.0	0.0076	3800
H	Hanochal	17	schist	64±4.4	0.023	3200

[a] Distance above confluence with Gilgit River
[b] Units are arbitrary - 100 is maximum for Schmidt hammer reading
[c] Measured locally (elevation change over ~250-500 m along river)
[d] Estimated for the mean annual peak discharge measured at Kachura gaging station (~146 km above Gilgit confluence)

Figure 10). These erosion rates are unusually rapid for a large bedrock river, and are thought to reflect rapid rock uplift, particularly along the Nanga Parbat - Haramosh Axis (Figure 10). Apatite and zircon fission track ages suggest denudation rates of this region up to ~cm/yr, with maximum rates located within the NPHA [Figure 8; *Burbank et al.*, 1996; *Zeitler*, 1985]. These apparently rapid river incision rates suggest this is an ideal site to study the processes of bedrock river incision, and to monitor erosion over a short time scale.

Our aim was to obtain first-order estimates of the 1) spatial and temporal variation of bed erosion rates, both at a site and over a ~150 km reach of the river; 2) erosion of the bed during "typical" flow conditions; and 3) variation in erosion rates through time, using erosion rates estimated over three timescales differing by several orders of magnitude. We measured erosion rates using two methods: 1) by drilling holes in the channel bedrock whose depth could be measured repeatedly to estimate the lowering of the surrounding rock surface over one year; and 2) by measuring cosmogenic radionuclide concentrations in rock collected from the bed of the river, providing an estimate of mean erosion rates over 1000's of years. To make these measurements, we selected accessible channel locations on the Indus 1) where substantial exposed bedrock extends from the low-flow river level to many meters above, allowing installation of drill holes and collection of cosmogenic radionuclide samples where maximum annual water depths reach up to ~10 m; 2) with a variety of bed morphologies, ranging from smooth rock to heavily ornamented surfaces etched by flutes and potholes; and 3) where sediment cover has likely been minimal through the recent past. Most of the seven sites chosen appear to be eroding primarily through abrasion, as joint spacing is sufficiently large to prevent quarrying. However, at sites C, D, and H, there is some evidence for at least occasional quarrying of blocks.

We documented the rock resistance, and the local channel geometry necessary to infer the stage history. At each site we measured channel cross sections and local (~0.5 km) river slope, noting the position and height of significant channel elevation drops and the elevation of a reddish stain line we infer reflects the mean high flow water level. Rock hardness was measured by using a Schmidt hammer test at each site [*Selby*, 1980], which measures rock compressive strength, a good surrogate for erosional resistance of rock [e.g., *Wohl et al.*, 1994]. Ten repeat measurements were made at each site, taking care to keep the hammer in a vertical orientation and to test spots away from discontinuities such as joints, fractures, and edges. These granites, schists, and gneisses are relatively resistant. Mean hammer test results from each site range from 56 to 69, and the hardness varies by only 10% among the seven sites (Table 1).

To estimate the typical hydrographic forcing and water coverage, we surveyed flow cross sections and slope at each site, and use flow records collected at the head of the Middle Gorge. Flow data were obtained from daily average flow records at the Kachura Bridge gauging station, collected from 1970 to 1986, which is near the upstream end of the Middle Gorge (~150 km upstream of the Gilgit River confluence, Figure 8). As the Indus River drainage area at

Figure 11. Example of drill hole placement (Site C, Figure 10). Flow is left to right, and reaches ~10 m depth during maximum flows. Note hole placement on smooth upstream faces (left of leftmost pen), and within flutes (between pencil and vernier caliper).

Kachura is ~100,000 km^2, and only relatively small tributaries enter the river within the Middle Gorge, it is likely that typical flows at each erosion site are well-represented by the measurements made at the Kachura station, despite the ~150 km length of the gorge We calculated the specific stream power (Eq. 3) using the average maximum daily discharge for an average year, and slopes measured using an inclinometer and laser rangefinder to measure elevation change over 100's of meters at each site (Table 1). We now discuss the specifics of the drill hole and cosmogenic radionuclide methods for measuring erosion rates.

3.1. Drill Hole Method

In Spring 1996, during low flow conditions, we drilled 3-9 holes in the channel floor in a variety of bed positions (Figure 11) at each of the seven sites. We selected the hole sites to capture the variation of erosion rates over short (meter) distances, where mean flow conditions, such as flow depth, sediment concentration, and total period of flow submersion, are likely similar, but local flow dynamics, such as streamline curvature, vary significantly. We drilled holes in local groups, located on the walls of flutes and potholes, as well as on the bed outside of such features (Figure 11). We used a hand held rock drill and rock hammer; holes were ~1.5-2.0 cm deep and ~0.5 cm wide, and ~1 to 6 m above the low flow river stage. We carefully cleaned sediment from each drill hole after installation, and then measured hole depth with a vernier caliper (Scienceware Type 6914) with a precision of ±0.05 mm. The depth was measured at the deepest portion of the hole, which was easily located because the drill bit produces a conical depression at the hole bottom. At least five repeat measurements were taken of each hole, with the micrometer consistently in the same orientation. Each hole was marked with the measurement orientation and a number, and then photographed.

During the peak flows in summer 1996, Indus River levels in the Middle Gorge reached roughly average maximum stage, based on anecdotal and photographic evidence (*D. Burbank*, pers. comm.; Figure 12). There is no evidence for unusually high or low flow conditions during this year. Given these flow conditions, the drill holes at the seven sites were under ~2-10 m of water at maximum discharges (~4250 m^3/sec). We reoccupied the drill hole sites in Spring 1997, and remeasured the hole depths following the procedure outlined above. We assume any decrease in hole depth reflects lowering of the bed around the hole by abrasion. We collected a sample from a

A.

B.

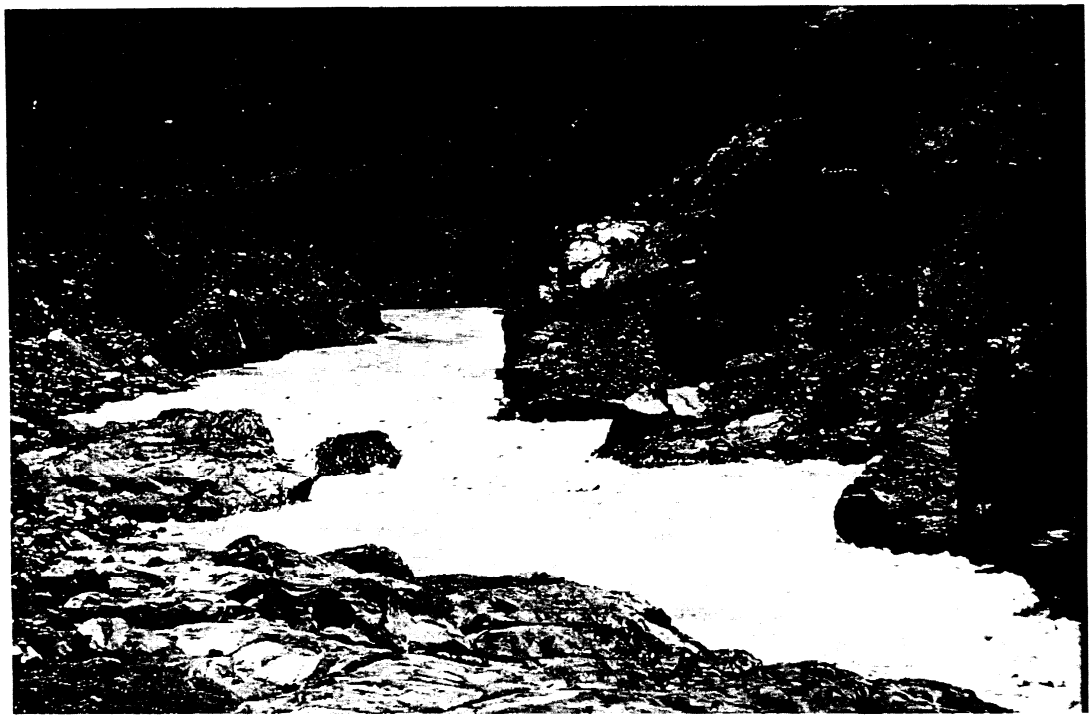

Figure 12. High and low flow photographs on the Indus River at Site H (Figure 10). Flow is toward the viewer. A) Site H shown at low flow conditions in April 1997. Discharge is ~300 m^3/sec. The drill hole and cosmogenic sample site is located on the platform near the center of the photo which juts into and constricts the flow. Flow width directly right of the platform is ~10 m. B) Site H shown at near mean annual flood in July 1996. Discharge is ~4200 m^3/sec, assuming flow is near mean annual maximum, which typically occurs at this time of year. At this stage, the platform on which the drill holes are located is buried by ~10-15 m of water.

slackwater deposit likely laid down during high flows in Summer 1996. Mean grain size from this deposit is ~1.9 ϕ (~0.27 mm, fine sand), and 80% of the grain size distribution falling between 2.5 ϕ to 1 ϕ (0.18 to 0.50 mm, fine to medium sand). This material is in suspension at high flows, and is likely the tool with which abrasion is accomplished. The hole depth changes are shown in Figure 13.

3.2. Cosmogenic Radionuclide Method

In order to estimate erosion rates on longer time scales, we utilize the newly evolved methods employing cosmogenic radionuclides (CRN). The concentration of radionuclides in a surface sample is used to infer the time the sample has taken to be exhumed through a production rate boundary layer of ~1-2 m. The erosion rates will therefore be average rates over this depth interval, assuming erosion is nearly steady. For example, if the true erosion rate is 1 mm/year, the measured rate will be averaged over ~1-2 ka. At several of the erosion sites, we collected samples to determine the concentration of the cosmogenic radionuclides (CRN) ^{10}Be and ^{26}Al in quartz within exposed bedrock. CRNs accumulate in a target mineral, such as quartz, through bombardment by secondary cosmic ray particles [see reviews in *Bierman*, 1994; *Nishiizumi et al.*, 1993], with the production rate P falling off exponentially below the surface. The concentration of CRNs, N, contained in a mineral now exposed at a surface which has been steadily eroding through time at a rate $\dot{\varepsilon}$ can be expressed as:

$$N = \frac{P_0 z^*}{\dot{\varepsilon} + \lambda z^*} \tag{14}$$

where P_0 is the CRN production rate at the rock surface, and z^* is the length scale for production attenuation as a function of depth ($z^*=\Lambda/\rho_r$, where Λ is the mean free path for the secondary cosmic ray particles, ~150 g/cm^2, and ρ_r is the rock density, ~2.7 g/cm^3). For rapid erosion rates (≥0.01 mm/yr), one may safely ignore radioactive decay. The above equation can then be rearranged to estimate the erosion rate, $\dot{\varepsilon}$,

$$\dot{\varepsilon} = \frac{P_0 z^*}{N} \tag{15}$$

where N is the measured CRN concentration.

We collected samples from bed locations that were well-exposed (i.e., no horizon blockage by local bed topography), near horizontal, and were adjacent to drill holes at all seven sites. Unfortunately, only three samples from these sites provided sufficient quartz for the CRN analysis. Maximum water depths over these sites range from ~2 to 10 m during a typical flow year. We estimated cosmic ray shielding from horizon blockage by measuring the angle to the skyline in 8 radial directions spaced by 45°, and using the equation of *Nishiizumi et al.* [1993]. We then calculate P_0 at each site by correcting the sea level, high latitude spallogenic production rate value of 21.29 atoms ^{27}Al/(g quartz - year) [*Clark et al.*, 1995] for the sample latitude and altitude using the production correction factors given in Table 2 of *Lal* [1991]. We neglect production of ^{27}Al by muon interactions, which should introduce negligible error at our sample elevation and latitude [*Brown et al.*, 1995].

At each site, we collected ~1 kg of rock, crushed the rock and extracted quartz. Typical quartz yields were ~50 g (Table 2), and ~1 g of ^{9}Be and ^{27}Al carrier was added to each sample. The quartz was purified and prepared for CRN isolation following the method of *Kohl and Nishiizumi* [1992]. Samples were analyzed for ^{10}Be/^{9}Be and ^{26}Al/^{27}Al ratios by accelerator mass spectrometry (AMS; *Elmore and Phillips*, 1987) at the Lawrence Livermore National Laboratory. Stable ^{27}Al concentrations in each sample were measured by ICP-MS at University of California - Santa Cruz. We were unable to obtain ^{10}Be/^{9}Be ratios, presumably due to very low concentrations in the quartz samples. However, we did obtain ^{26}Al/^{27}Al ratios, and used the measured ^{27}Al concentration in each sample to determine the concentration of the cosmogenic ^{26}Al (Table 2).

While CRNs have been used for inferring long term erosion rates in a number of geomorphic settings, as far as we know, this has never been attempted on an actively eroding river bed. There are several complexities to consider when interpreting the CRN concentrations obtained from samples collected from an active river bed. The surface production rate, P_0, could vary with time by: 1) variation in blockage of CRN production (lowering of P_0) during the year by water coverage; 2) variation in shielding produced by differential lowering of local bed topography surrounding the sample site; and 3) periodic burial of the bed by sediment. In addition, the steady state erosion assumption of Eq. 15 could be violated by non-steady

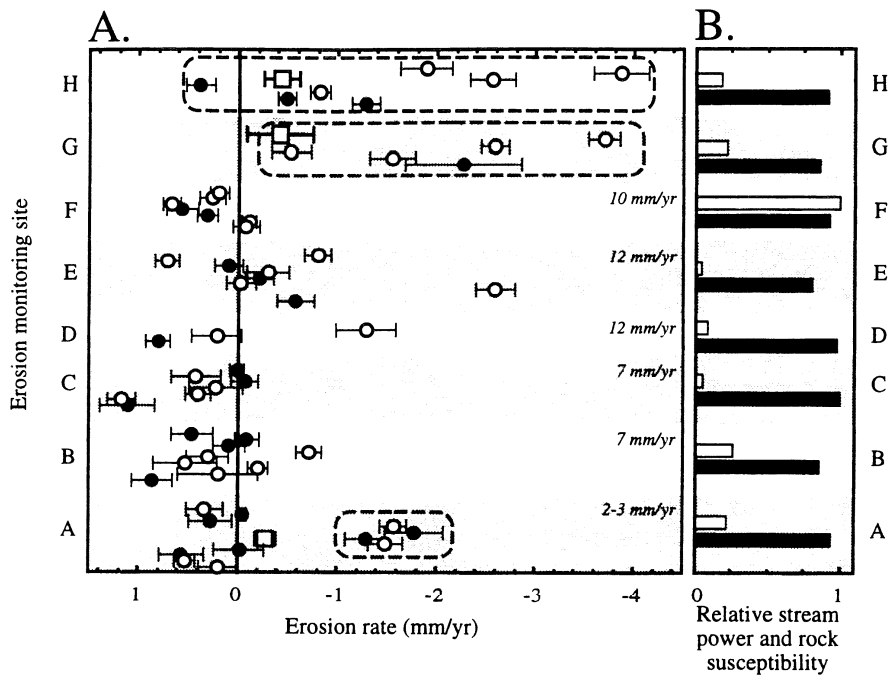

Figure 13. A) Erosion measurement results. On graph, open circles show depth changes for drill holes installed within flutes and potholes, and solid circles for drill holes placed outside of such forms (see Figure 11). The drill hole depth changes are obtained by subtracting the mean hole depth obtained from 5 measurements in 1997 by the results of the same measurements made in 1996, and error bars on drill hole measurements correspond to propagation of 1s errors obtained from these measurements. The open boxes are the erosion rates estimated using the concentration of ^{26}Al in rock collected from the bed surface at each site, using Eq. 15, and 1s error bars reflect propagation of all analytical and CRN production rate errors. The dashed circles enclose drill holes installed in locally narrow and steep (i.e., high energy expenditure) channel segments. Numbers on right side of graph correspond to long-term erosion rates estimated from the strath terraces dated by *Burbank et al.*, 1996 nearest to each site. B) Relative stream power (hollow bars) and rock susceptibility (solid bars - inferred from Schmidt hammer tests) for each site.

erosion of the bed. Of these potential complicating factors, only the sample site coverage by water can be constrained quantitatively with available data. We have chosen our sampling sites to minimize the problems associated with the other complexities.

We calculate CRN production shielding by water coverage using measured flow data to estimate flow depths over each site. As CRN production decays exponentially with depth, z, in material, $P=P_0e^{(-z/z^*)}$ (z^*=~1.6 m for water), we require a history of water depth above each sample site. First, we establish a rating curve (flow depth vs. discharge) for each river cross section at which a sample was collected. To do so, we use the surveyed cross section and local slope, and input these into the Manning equation to calculate mean flow velocity at each flow depth (Figure 14). We compiled the minimum, average, and maximum daily flow for each day of the year from the data collected at the Kachura gauging station. We take the red stain line to reflect the average high flow, which is supported by high flow observations in summer 1996 [*D. Burbank*, pers. comm., 1996]. Second, using the rating curve, we estimate the discharge at which the CRN sample site first becomes covered. We use the rating curve and daily flows to yield a graph of flow depth above the sample site through the year (Figure 14). We then integrate the daily production rate over a year, and obtain the annual production rate in the face of water shielding. Annual production rates calculated by this method tend to be 75-95% of the uncovered production rates (Figure 14), despite burial of these sampling sites by up to ~10 m of water during high flows. The small magnitude of the correction reflects the small portion of the year during which high flows occur on the Indus.

The variation in shielding associated with local bed topography evolution, and with possible temporary burial by sediment, are more difficult to constrain. The effect of shielding would tend to lower the average production rate experienced by the sample. As with water shielding,

Table 2. Cosmogenic radionuclide results.

Site	Altitude (m)	Latitude	Sample thickness (cm)	Horizon shielding correction[a]	Water shielding correction[b]	Total quartz extracted (g)	^{26}Al concentration (atoms/mg)[c]	Exposure age (yr)[d]	Erosion rate (mm/yr)[d]
A	2099	35.3	5	0.92	0.95	56.5408	2.84±1.0	2560±1000	0.230±0.086
G	1440	35.8	5	0.88	0.75	51.4326	1.80±1.4	1700±1400	0.347±0.28
H	1300	35.8	5	0.90	0.75	50.3467	1.33±0.5	1640±710	0.375±0.16

[a] Calculated according to procedure of Nishiizumi et al. (1993)
[b] Calculated using average annual hydrograph to estimate sample site coverage (see text)
[c] ^{10}Be samples yielded no measurable values for these locations
[d] Calculated using a latitude and altitude corrected production rate of 29.21 atoms ^{26}Al/(g quartz - yr) (Lal, 1991, Table 2; Clark et al., 1995)

neglect of past topographic shielding therefore results in an overestimate of the average erosion rate, $\dot{\varepsilon}$. In an effort to avoid periodic burial by sediment, we collected from sites that are currently devoid of sediment and are not in topographic depressions on the bed. The collection sites are in narrow, bedrock reaches that we feel are not likely to be covered with sediment often. We therefore assume that errors introduced by periodic sediment burial are insignificant.

Non-steady erosion effects should also introduce negligible error into the estimated erosion rates. The steady erosion assumption underlying Eq. 15 could be tested by using the ratio of ^{26}Al/^{10}Be and the "banana" diagram [Fig. 5, *Lal*, 1991; Fig. 3, *Nishiizumi et al.*, 1993]. Unfortunately, in this study, ^{10}Be results were below detection limits, precluding the use of this test. However, we first consider a non-steady scenario where erosion is periodic, with each erosion episode nearly instantaneously (relative to 1000's of years) removing an equal thickness from the bed, and no bed lowering otherwise, as carefully considered by *Small et al.* [1997]. If these erosional episodes are very frequent, instantaneous rates must be only slightly greater than the long term erosion rate; this scenario effectively collapses to the steady assumption of Eq. 15 [*Small et al.*, 1997]. However, even for low frequency events, we can constrain the error. For example, a ~1 m block quarried once every ~1000 years with negligible erosion otherwise ($\dot{\varepsilon}$=~1 mm/yr), the analysis of *Small et al.* [1997] suggests an erosion rate estimated using CRNs off by at most ±~50% from the true mean erosion rate for that spot. While bed erosion in a river is likely episodic, erosional episodes may not be equal. However, if erosion in these episodes varies over a range of approximately of the order of the long term erosion rate, erosion rates estimated with CRNs using Eq. 15 should again approximate well the long-term average rate. The erosion rates estimated with CRNs, using Eq. 15, are shown with the drill hole results in Figure 13. Error bars represent primarily analytical and production rate errors; no attempt is made to correct for possible non-steady erosion.

3.3. Discussion of Erosion Measurements

We first discuss the changes in the drill hole depth between 1996 and 1997, shown on Figure 13. There were several holes (at sites A and H) that spawned small flutes trailing off of their downstream side (Figure 15). These flutes had widths of about the hole diameter, maximum depths of up to ~1 cm, and lengths of ~2 cm. The generation of these small flutes clearly demonstrates that the holes influenced local flow conditions, and illustrates the critical role of local bed perturbations in focusing erosion. We took care not to include the spawned flutes in the measurements of bed lowering around the holes. Many of the holes were partially to fully filled with fine to coarse sand, with some grains nearly equal in size to the hole diameter tightly lodged in the hole. None of the bed surfaces around the drill holes were covered by more than ~1 cm of sand. In most cases, our measurements of drill hole depth changes reflect the lowering of the bed around the drill hole, rather than lowering of the hole opening only. We realize that several of the holes actually appeared to deepen (depth changes are positive, Figure 13). This likely results either from deepening of the holes accidentally while we attempted to clean them of sediment in 1997, or from an improvement in our hole cleaning technique in 1997. It seems unlikely that the hole bottoms were lowered selectively, given their high aspect ratio and narrow diameter. At worst, all of the bed lowering measurements may be considered underestimates of the actual bed lowering, by ~0.5 mm. We believe that the measured bed lowering is the direct result of abrasion, which we infer because 1) chatter marks and chips made in the rock during drill hole installation have been significantly smoothed, suggesting polishing by abrasion (rather than cavitation); 2) quarrying appears to operate on larger scales; and 3) the highest erosion rates are found in abrasional forms, like flutes.

The drill-hole bed lowering measurements reveal that erosion rates are highly variable both between and within sites (Figure 13). In several locations (sites B, C, and F),

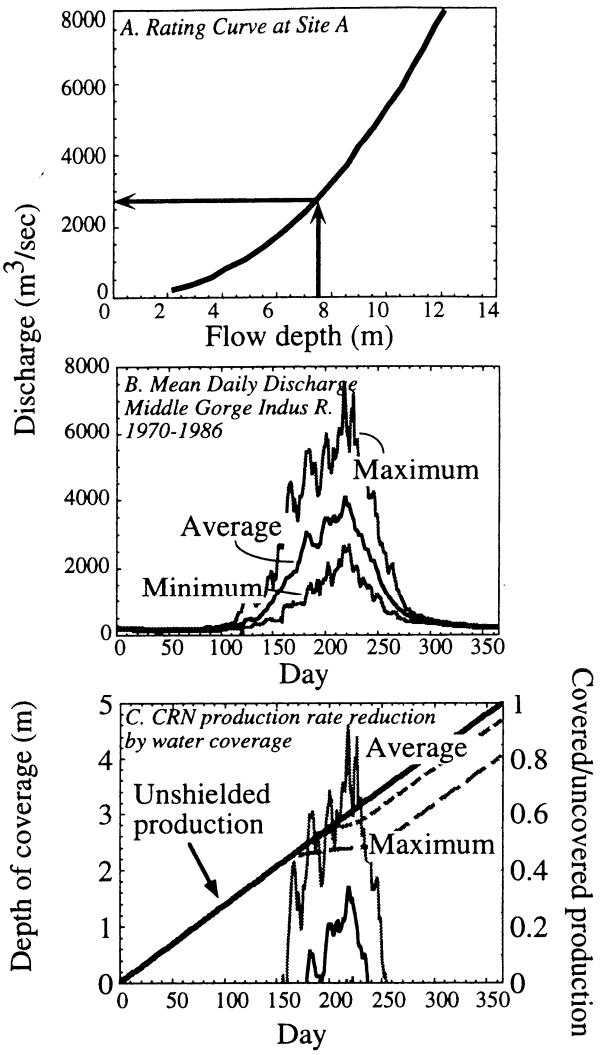

Figure 14. Example of correction of CRN erosion rate for water shielding, performed for Site A (Figure 10). We seek a history of water depth above the site to estimate the shielding. A) Rating curve for the site, relating flow depth to discharge. B) The maximum, average, and minimum historical mean daily flows for each Julian day recorded at Kachura gauging station, 1970 and 1986. C) Daily water depth above CRN sample site obtained from historical daily average flows (thin black line) and maximum flows (thin gray line) obtained by using the discharge data presented in B to determine flow depth with rating curve in A. Mean minimum daily flows are insufficient to cover site. The thick line tracks the relative accumulation of CRNs on the bed assuming no water shielding; the slope of this line is the relative unshielded production rate, $P_0/[P_0(365$ days)]. The dashed lines track CRN accumulation in the face of water shielding by the average and maximum flows; the slopes of these lines are the instantaneous relative production rate, $P_0e^{(-H/z^*)}/[P_0(365$ days)], where H is the flow depth. The slopes of the dashed are lower than the solid, unshielded line when the site is covered by water, reflecting lowered production rates. The right axis shows the relative annual production rate, with a value of 1 equivalent to the unshielded rate. The production rates on the bed surface are lowered by ~5-20% relative to the unshielded production rate.

there appears to be no appreciable bed lowering over the Spring 1996 to Spring 1997 interval. At the remaining sites, maximum bed lowering rates range from ~1 to 4 mm; the maxima are typically within flutes (open circles, Figure 13). The maximum bed lowering rates of ~4 mm/yr was measured in a flute of ~10 cm maximum depth. Remarkably, at these rates, flutes like those in Figure 3 may require only a few 10's of years to evolve, particularly if erosion rates increase nonlinearly with discharge. Importantly, erosion rate variations do not appear to reflect rock hardness variations. While erosion rates vary by about an order of magnitude, the Schmidt hammer tests vary by only ~10%, suggesting that the abrasional resistance of these rocks at each site are comparable (Table 1; Figure 13). Abrasional wear therefore must reflect instead variations in the local flow field.

The measured rates are highest where channel width decreases and/or slope increases to produce channel segments of locally high energy expenditure. The holes with the highest erosion rates are within short reaches of steep elevation drops and channel narrowing (holes at sites A, G, and H, enclosed by dashed circles, Figure 13). We infer from this that erosion rates are greatest where stream power (Eq. 3) is locally high. In contrast, reach-averaged stream power estimates for each site, calculated using slopes averaged over 100's of meters comparable to those one would obtain from maps and similar to the length scales used in channel erosion rules (Eq. 7), fail to predict well the locations of most rapid bed lowering (Figure 13). For example, site F, with the highest reach-averaged stream power, showed no abrasion during our monitoring. This points out a significant problem with trying to apply reach-averaged slopes to predict bedrock erosion rates, as in Eq. 7, particularly given the strong erosion rate dependence on channel slope in the rate-predicting rules discussed in section 2.

The CRN estimated erosion rates of ~0.25-0.50 mm/yr at sites A, G, and H are several times lower than the maximum bed lowering rates obtained from the drill holes (Figure 12, squares). We report as well one other CRN measurement on the bed at site F, which yields a similar rate [*J. Leland*, pers. comm., 1997]. These rates are very low compared to the drill hole measurements at each site (except site F). Comparison of the CRN rates, which effectively average bed lowering rates over ~1.5 to 2 ka, to the annual rates obtained from the drill holes implies that bed erosion rates at a point on the bed must vary

Figure 15. Drill holes in a flute at Site H, showing small flutes generated on the downstream edge of both holes. Flow is from left to right. The flute on hole 6 is the more visible. The drill hole is located just above the "6", with two black lines on either side. Hole diameter is ~0.5 cm. The flute extends upward and to the right for ~5 cm, and is ~0.5 cm deep, and shallows away from the hole.

significantly through time. If bed erosion is accomplished by abrasion, the loci of bed erosion may move as active flutes migrate across the bed surface, and as potholes are born and die, as outlined in Section 2.1.3 above. This implies erosion by abrasion is episodic at any single point on the bed, with much of the erosion accomplished within flutes and potholes, where suspended sediment efficiently delivers kinetic energy through impact.

Reconciliation of our measurements with the rates of *Burbank et al.* [1996] is also needed. The much higher long-term rates obtained from the strath terraces may reflect hydrologic and/or sediment supply changes in the Indus River system during the ~6 to 70 ka since terrace abandonment that allowed incision rates to be at times much higher than present. Glacial/interglacial climate cycling provides one possible explanation. In this scenario, changes in the frequency or magnitude of discharge and/or of the sediment supply alter erosion rates. Our lower annual (drill hole) and millennial (CRNs) erosion rates may reflect modern and recent (last ~2 ka) flow and sediment supply conditions that are unlike those that accomplished much of the bed lowering since abandonment of the straths. We hypothesize that during glacial or glacial/interglacial transitions, the magnitude and/or frequency of discharge and sediment conditions favorable for bed erosion were greater, resulting in bed erosion rates higher than at present. This scenario has been suggested for other river systems [e.g., *Foley*, 1980b], and requires that incision rates on the Indus during these periods are even higher than the remarkably high long-term average rates obtained by *Burbank et al.* [1996].

Another alternative explanation is that we have measured rates of the wrong process. Perhaps quarrying of the bed is the primary mechanism by which the river is incising, over the long term. As outlined in Section 2.2, quarrying is likely to be a more efficient erosional process where it can be active. To account for the long-term average erosion rates, quarrying must currently act in locations within the channel we have not measured, or was active prior to the time period covered by our mean erosion rates (~1 to 2 ka). Both seem unlikely at our sites, because joint spacing seems sufficiently large to prevent quarrying. We can, however, also consider the possibility that quarrying is active in the very sites we have measured. To do so, we interpret our CRN concentrations as exposure ages ($t=N/P_0$) of ~1.5 to 2 ka, assuming essentially no surface erosion;

these "ages" are interpreted to reflect the period of time elapsed since the last quarrying episode. Reconciliation of the "waiting times" with the long-term erosion rates of ~2 to 10 mm/yr *Burbank et al.* [1996] requires blocks or many blocks totaling ~3 to 20 m were quarried during the last quarrying episode. While we see no evidence of this, it is nonetheless difficult to rule out.

4. SYNTHESIS

Bedrock channels erode and evolve through an interconnected set of erosion processes. Our observations indicate that the primary mechanisms in hard bedrock are abrasion by suspended load and quarrying of blocks from the bed. Quarrying is the more efficient of these processes, and, where joint spacing allows, accomplishes much of the incision in a bedrock river channel. However, more massive rocks require cutting by abrasion. As this process is less efficient, in order to maintain a steady profile, a river must become steeper and/or narrower relative to quarried reaches, providing sufficient energy to allow abrasion to keep pace. Such reaches often appear to form local base-level for the upstream reach, which may have the potential to erode more rapidly through plucking; if true, reaches where abrasion is the primary tool may limit the rate at which a river slices through underlying bedrock.

Abrasion rates are very sensitive to the local flow velocity, and our bedform observations and measurements suggest it is most effectively accomplished by the suspended load. A simple scaling rule, developed following *Foley* [1980a] and *Anderson* [1986], implies $dz/dt \propto v_w^5$. Abrasion is most effective where sediment can be "flung" forcefully from the flow, and we argue this occurs in regions of separated flow, which generate high flow curvature. Flutes and potholes, which our measurements show are places of most active abrasion, are formed in and enhance flow separation. Since sediment must be entrained and carried into these forms, and the surfaces of these features are typically smooth rather than chipped and chatter marked, the effective abrasive impacts are delivered by the suspended load.

Quarrying appears to be the most efficient process where it is active. The process removes material from the bed by removing joint-defined blocks, either by lift or sliding. Our scaling rules imply the capacity of a flow to quarry blocks goes as $\sim v_w^2$; again, a nonlinear process. Typical flows on the Indus River are capable of generating lift to quarry blocks of ~0.7 m thickness, and of sliding blocks up to ~0.15 m, given the assumptions in our calculations. However, erosion by the quarrying process likely requires a "waiting period" to allow blocks to be loosened by subaerial weathering, bashing by bedload, or widening by a previously undocumented process, hydraulic wedging. Hydraulic wedging refers to the forcible emplacement of rocks into a joint, possibly during slight joint widening in response to turbulent pressure fluctuations within the flow. In this way, hydraulic wedging acts to ratchet open the joint, assisting in preparing the block to be quarried, both directly and by enhancing weathering rates in the widened crack.

Cavitation is not a significant erosive mechanism in natural bedrock channels we have investigated. Evidence for cavitation, such as small-scale surface pitting, has not been confidently identified on the bed of these channels. The flow conditions necessary for cavitation to occur require very high velocities for a given flow depth, and, hence, the water surface slope must be quite high to exceed the threshold for cavitation. Even on the Indus, a high discharge and steep channel, cavitation appears possible only at the most extreme high flows. Locally steep segments of bedrock river channels with water slopes high enough to generate the velocities necessary for cavitation are also typically locations where flow aeration is greatest. Introduction of even relatively small amounts of entrained air into the flow can reduce cavitation to a negligible or nonexistent process.

Through development of simple scaling rules for each of the major channel eroding processes (abrasion, quarrying, and cavitation), we find a strong dependence of process rate on local flow conditions. Each of the scaling rules indicate a nonlinear dependence of process rate on velocity, with powers of ~2 to 5. Our measurements of abrasion on the bed of the Indus quantitatively support the importance of local flow conditions for setting erosion rates.

Erosion rates measured with drill hole depth changes on the bed of the Indus River are remarkably variable in space, and reflect local variations in both flow dynamics and energy expenditure. Our annual (drill hole) bed lowering rates vary from ~0 to ~4 mm/yr, with these rates varying both within and between the seven monitoring sites. Miniature flutes with depths up to ~1 cm and similar in form to those shown in Figure 3, were spawned on several holes, confirming the ability of bed perturbations to enhance dramatically local bed erosion through alteration of the water flowlines. Consistent with this idea, the highest drill hole erosion rates are typically within flutes and potholes. Nearly all of the most rapid measured bed lowering took place within channel segments of a few 10's of meters length that were narrower and steeper, and with correspondingly greater energy expenditure, than was typical for the reach. Taken together, these results imply local variations in flow dynamics and energy expenditure are perhaps the most critical factors in setting erosion rates, at least by abrasion, and that these variables must be considered meaningfully when constructing reach-scale rules for bedrock erosion.

The differences in mean erosion rates obtained from drill holes (annual), CRN bed measurements (~1.5 to 2 ka), and long-term strath terrace dates (~6-70 ka) are up to ~2 orders of magnitude. The CRN bed measurements are several times lower at 3 sites (A, G, and H) than the maximum drill hole measurements. This is consistent with our

conceptual idea that flutes, which with potholes are the locations of the most rapid bed abrasion, migrate across the bed, and are separated by more slowly eroding to non-eroding bed surfaces. These "dead" surfaces wait until the next flute is generated or migrates past, and long-term erosion rates measured with CRNs integrate this "waiting time" between form passage, and are therefore necessarily lower than the maximum drill hole rates. The typical spacing between forms is consistent with the ten-fold difference between drill holes measurements and the CRN bed erosion measurements. All of our measured erosion rates, however, are substantially lower than the rates estimated from strath terraces [*Burbank et al.*, 1996] near these locations. These higher long-term rates require erosion to have been higher in the past, possibly during glacial times or glacial/interglacial transitions, when larger and/or more frequent high discharges coupled with more available erosive tools likely provided the river with more capacity for bed erosion. An alternative is that we have missed the relevant process by focusing on abrasion. Quarrying of blocks may be the more efficient process. If so, it must be currently active elsewhere in the channel if quarrying is presently eroding the bed at the rates of *Burbank et al.* [1996]. If quarrying were to be the dominant process at our CRN measurement sites, interpreting the CRN concentrations as "waiting times" since the last quarrying event requires that ~3 to 20 m of total lowering by block removal took place at ~1.5 to 2 ka to produce erosion rates comparable to *Burbank et al.* [1996]. We would argue that this is less likely, and that the discrepancy instead reflects true variation in erosion rates, associated with hydrologic changes, in the reaches on which we have focused.

Acknowledgments. Funding for this project has been provided by National Science Foundation grant EAR-9417798 (to RSA and KXW), and an IGPP Award from Lawrence Livermore National Labs (to RSA). We thank J. Khan, A. Khan, D. Burbank, G. Pratt, A. Felton, and E. Small for help in lab, field and writing, and to E. Wohl and K. Tinkler for organizing the conference leading to this volume. We greatly appreciate the insightful comments on the manuscript provided by G. Pickup and J. Costa. Many thanks are also given to the wonderful people of the Indus River Middle Gorge - their curiosity and kindness are unforgettable.

REFERENCES

Alexander, H.S., Pothole erosion, *.l Geol., 40*, 335-347, 1932.

Allen, J.R.L., Flute marks and flow separation, *Nature, 219*, 602-604, 1968.

Allen, J.R.L., Transverse erosional marks of mud and rock: their physical basis and geological significance, *Sed. Geol., 5* (3/4), 167-370, 1971.

Anderson, R.S., Erosion profiles due to particles entrained by wind: Application of an eolian sediment transport, *Geol. Soc. Amer. Bull., 97*, 1270-1278, 1986.

Ashley, G.M., W.H. Renwick, and G.H. Haag, Channel form and processes in bedrock and alluvial reaches of the Raritan River, New Jersey, *Geology, 16*, 635-646, 1988.

Barnes, H.L., Cavitation as a geological agent, *Amer. J.Sci., 254*, 493-505, 1956.

Bierman, P.R., Using in situ produced cosmogenic isotopes to estimate rates of landscape evolution: A review from the geomorphic perspective, *J. Geophys. Res., 99* (B7), 13885-13896, 1994.

Bourne, N.K., and J.E. Field, A high-speed photographic study of cavitation damage, *J. Appl. Phys., 78* (7), 4423-4427, 1995.

Brown, E.T., D.L. Bourles, F. Colin, G.M. Raisbeck, F. Yiou, and S. Desgarceaux, Evidence for muon-induced production of 10Be in near-surface rocks from the Congo, *Geophys. Res. Lett., 22* (6), 703-706, 1995.

Burbank, D.W., J. Leland, E. Fielding, R.S. Anderson, N. Brozovic, M.R. Reid, and C. Duncan, Bedrock incision, rock uplift and threshold hillslopes in the northwestern Himalayas, *Nature, 379*, 505-510, 1996.

Chadwick, O.A., R.D. Hall, and F.M. Phillips, Chronology of Pleistocene glacial advances in the Central Rocky Mountains, *Geol. Soc. Amer. Bull., 109* (11), 1443-1452, 1997.

Clark, D.H., P.R. Bierman, and P. Larsen, Improving in situ cosmogenic chronometers, *Quat. Res. (New York), 44* (3), 367-377, 1995.

Costa, J.E., and J.E. O'Connor, Geomorphically effective floods, in *Natural and anthropogenic influences in fluvial geomorphology: The Wolman volume: Geophysical Monograph 89*, edited by J.E. Costa, A.J. Miller, K.W. Potter, and P.R. Wilcock, pp. 45-56, American Geophysical Union, Washington, D.C., 1995.

Elmore, D., and F. Phillips, Accelerator mass spectrometry for measurement of long-lived radioisotopes, *Science, 236*, 543-550, 1987.

England, P.C., and P. Molnar, Surface uplift, uplift of rocks, and exhumation of rocks, *Geology, 18* (12), 1173-1177, 1990.

Foley, M.G., Bed-rock incision by streams, *Geol. Soc. Am., Bull., 91* (10), I 577-I 578, II 2189-II 2213, 1980a.

Foley, M.G., Quaternary diversion and incision, Dearborn River, Montana, *Geol. Soc. Am., Bull., 91* (10), I 576-I 577, II 2152-II 2188, 1980b.

Greeley, R., and J.D. Iversen, Wind as a geological process on Earth, Mars, Venus and Titan, *Cambridge Planetary Science Series*, 333, 1985.

Hammitt, F.G., *Cavitation and Multiphase Flow Phenomena*, 423 pp., McGraw-Hill, Inc., New York, 1980.

Hancock, G.S., R.S. Anderson, O.A. Chadwick, and R.C. Finkel, Dating fluvial terraces with ^{10}Be and ^{26}Al profiles: Application to the Wind River, Wyoming, *Geomorphology*, in press, 1998.

Howard, A.D., Modelling fluvial systems; rock-, gravel- and sand-bed channels, *Special Publication Inst. Brit. Geogr., 18*, 69-94, 1987.

Howard, A.D., A detachment-limited model of drainage basin evolution, *Water Resour. Res., 30* (7), 2261-2285, 1994.

Howard, A.D., W.E. Dietrich, and M.A. Seidl, Modeling fluvial erosion on regional to continental scales, *J. Geophys. Res., B, Solid Earth and Planets, 99* (7), 13,971-13,986, 1994.

Howard, A.D., and G. Kerby, Channel changes in badlands, *Geol. Soc. Amer. Bull., 94* (6), 739-752, 1983.

Knighton, D., *Fluvial forms and processes*, 218 pp., Edward Arnold, London, 1984.

Kohl, C.P., and K. Nishiizumi, Chemical isolation of quartz for measurement of *in-situ* -produced cosmogenic nuclides, *Geochim. Cosmochim. Acta, 56*, 3583-3587, 1992.

Lal, D., Cosmic ray labeling of erosion surfaces: in situ nuclide production rates and erosion models, *Earth Planet. Sci. Lett., 104*, 424-439, 1991.

Leopold, L.B., M.G. Wolman, and J.P. Miller, Fluvial processes in geomorphology, W.H.Freeman, San Frncisco, 1964.

Maxson, J.H., and I. Campbell, Fluting and facetting of rock surfaces, *J. Geol., 48*, 717-751, 1940.

Miller, J.R., The influence of bedrock geology on knickpoint development and channel-bed degradation along downcutting stream in south-central Indiana, *J. Geol., 99*, 591-605, 1991.

Nemec, W., M.N. Lorenc, and J. Saavedra, Potholed granite terrace in the Rio Salor Valley, western Spain: a study of bedrock erosion by floods, *Techniterrae*, 6-21, 1986.

Nishiizumi, K., C.P. Kohl, J.R. Arnold, R.I. Dorn, J. Klein, D. Fink, R. Middleton, and D. Lal, Role of in situ cosmogenic nuclides ^{10}Be and ^{26}Al in the study of diverse geomorphic processes, *Earth Surf. Proc. Land., 18*, 407-425, 1993.

Rosenbloom, N.A., and R.S. Anderson, Hillslope and channel evolution in a marine terraced landscape, Santa Cruz, *J. Geophys. Res., 99* (B7), 14013-14029, 1994.

Seidl, M.A., and W.E. Dietrich, The problem of channel erosion into bedrock, *Catena Supplement, 23*, 101-124, 1992.

Seidl, M.A., W.E. Dietrich, and J.W. Kirchner, Longitudinal profile development into bedrock; an analysis of Hawaiian channels, *J. Geol., 102* (4), 457-474, 1994.

Selby, M.J., A rock mass strength classification for geomorphic purposes: with tests from Antartica and New Zealand, *Zeit. Geomorph. N.F. Band 24*, 31-51, 1980.

Sklar, L., and W.E. Dietrich, The influence of downstream variations in sediment supply and transport capacity on bedrock channel longitudinal profiles, *Eos, Trans. AGU, 78*, F229, 1997.

Slingerland, R., S.D. Willet, and H.L. Hennessey, A new fluvial bedrock erosion model based on the work-energy principle, *EOS Supplement, 78*, F299-F300, 1997.

Small, E.E., and R.S. Anderson, Geomorphically driven late Cenozoic rock uplift in the Sierra Nevada, California, *Science, 270* (5234), 277-280, 1995.

Small, E.E., R.S. Anderson, J.L. Repka, and R. Finkel, Erosion rates of alpine bedrock summit surfaces deduced from in situ 10Be and 26Al, *Earth Planet. Sci. Lett., 150* (3-4), 413-425, 1997.

Stock, J.D., and D.R. Montgomery, Can we predict the rate of bedrock river incision (using the stream power law)?, *J. Geophys. Res.*, in press.

Suzuki, T., and K. Takahashi, An experimental study of wind abrasion, *J. Geol., 89* (1), 23-36, 1981.

Tinkler, K.J., Fluvially sculpted bedforms in Twenty Mile Creek, Niagara Peninsula, Ontario, *Can. J. Earth Sci., 30*, 945-953, 1993.

Tucker, G.E., and R. Slingerland, Drainage basin responses to climate change, *Water Resour. Res., 33* (8), 2031-2047, 1997.

Wohl, E.E., Bedrock benches and boulder bars; floods in the Burdekin Gorge of Australia [with Suppl. Data 92-14], *Geol. Soc. Amer. Bull., 104* (6), 770-778, 1992.

Wohl, E.E., Bedrock channel incision along Piccaninny Creek, Australia, *J. Geol., 101* (6), 749-761, 1993.

Wohl, E.E., N. Greenbaum, A.P. Schick, and V.R. Baker, Controls on bedrock channel incision along Nahal Paran, Israel, *Earth Surf. Proc. Land., 19* (1), 1-13, 1994.

Wolman, M.G., and J.P. Miller, Magnitude and frequency of forces in geomorphic processes, *J. Geol., 68* (1), 54-74, 1960.

Zeitler, P.K., Cooling history of the NW Himalaya, Pakistan, *Tectonics, 4* (1), 127-151, 1985.

Zen, E.A., and K.L. Prestegaard, Possible hydraulic significance of two kinds of potholes; examples from the paleo-Potomac River, *Geology, 22* (1), 47-50, 1994.

Gregory S. Hancock, Dept. of Earth Sciences and Institute of Tectonics, University of California, Santa Cruz, CA, 95064, ghancock@bagnold.ucsc.edu.

Robert S. Anderson, Dept. of Earth Sciences and Institute of Tectonics, University of California, Santa Cruz, CA, 95064, rsand@bagnold.ucsc.edu.

Kelin X Whipple, Dept. of Earth, Atmospheric, and Planetary Sciences, Massachusetts Instiute of Technology, Cambridge, MA, 02138, kxw@mit.edu.